

# **SEMI-EMPIRICAL PROCEDURES FOR EVALUATING LIQUEFACTION POTENTIAL DURING EARTHQUAKES**

by

**I. M. Idriss and R. W. Boulanger**  
**Department of Civil & Environmental Engineering**  
**University of California, Davis, CA 95616-5924**  
*e-mail: [imidriss@aol.com](mailto:imidriss@aol.com) & [rwboulanger@ucdavis.edu](mailto:rwboulanger@ucdavis.edu)*

**Invited Paper**

**Presented at**

**The Joint**

**11<sup>th</sup> International Conference on Soil Dynamics & Earthquake Engineering  
(ICSDEE)**  
**and**  
**The 3<sup>rd</sup> International Conference on Earthquake Geotechnical Engineering  
(ICEGE)**

**January 7 – 9, 2004**

**Berkeley, California, USA**

**Proceedings of the 11<sup>th</sup> ICSDEE & 3<sup>rd</sup> ICEGE  
pp 32 – 56**

# Semi-empirical Procedures for Evaluating Liquefaction Potential During Earthquakes

I. M. Idriss<sup>1</sup>, R. W. Boulanger<sup>1</sup>

<sup>1</sup>Department of Civil & Environmental Engineering, University of California, Davis, CA

*Abstract*—Semi-empirical procedures for evaluating the liquefaction potential of saturated cohesionless soils during earthquakes are re-examined and revised relations for use in practice are recommended. The stress reduction factor ( $r_d$ ), earthquake magnitude scaling factor for cyclic stress ratios ( $MSF$ ), overburden correction factor for cyclic stress ratios ( $K_\sigma$ ), and the overburden normalization factor for penetration resistances ( $C_N$ ) are discussed and recently modified relations are presented. These modified relations are used in re-evaluations of the SPT and CPT case history databases. Based on these re-evaluations, revised SPT- and CPT-based liquefaction correlations are recommended for use in practice. In addition, shear wave velocity based procedures and the approaches used to evaluate the cyclic loading behavior of plastic fine-grained soils are discussed.

*Keywords*—Liquefaction, SPT, CPT, earthquakes.

## INTRODUCTION

Semi-empirical field-based procedures for evaluating liquefaction potential during earthquakes have two essential components: (1) the development of an analytical framework to organize past case history experiences, and (2) the development of a suitable in-situ index to represent soil liquefaction characteristics. The original simplified procedure (Seed and Idriss 1971) for estimating earthquake-induced cyclic shear stresses continues to be an essential component of the analysis framework, although there have been a number of refinements to the various components of this framework. Other major developments in the past thirty years have included improvements in the in-situ index tests (e.g., SPT, CPT, BPT, shear wave velocity), and the continued collection of liquefaction/no-liquefaction case histories.

The strength of the semi-empirical approach is the use of theoretical considerations and experimental findings to establish the framework of the analysis procedure and its components. Sound theory provides the ability to make sense out of the field observations, tying them together, and thereby having more confidence in the validity of the approach as it is used to interpolate or extrapolate to areas with insufficient field data to constrain a purely empirical solution. Purely empirical interpretations of the field case histories, without any physics-based framework, would leave unclear the conditions for which the empirical relations truly are applicable. For example, the purely

empirical derivations of individual factors of the analysis method (e.g., an  $MSF$ ,  $r_d$ , or  $K_\sigma$  relation) are complicated by their dependence on other components of the analysis method, and thus a purely empirical derivation is often not well constrained by the available case history data.

This paper provides an update on the semi-empirical field-based procedures for evaluating liquefaction potential of cohesionless soils during earthquakes. This update includes recommended relations for each part of the analytical framework, including the:

- stress reduction coefficient  $r_d$ ,
- magnitude scaling factor  $MSF$ ,
- overburden correction factor  $K_\sigma$  for cyclic stress ratios, and
- overburden correction factor  $C_N$  for penetration resistances.

For each of these parameters, the emphasis has been on developing relations that capture the essential physics while being as simplified as possible. These updated relations were then used in re-evaluations of the field case histories to derive revised deterministic SPT-based and CPT-based liquefaction correlations. Lastly, shear wave velocity ( $v_s$ ) based liquefaction correlations and the procedures for evaluating the cyclic loading behavior of plastic fine-grained soils are discussed briefly.

## OVERVIEW OF THE FRAMEWORK USED FOR SEMI-EMPIRICAL LIQUEFACTION PROCEDURES

A brief overview is provided for the framework that is used as the basis for most semi-empirical procedures for evaluating liquefaction potential of cohesionless soils during earthquakes. This overview provides the context in which the  $r_d$ ,  $MSF$ ,  $K_\sigma$ , and  $C_N$  relations are derived and used. Each of these factors is then revisited in subsequent sections.

### *The Simplified Procedure for Estimating Cyclic Shear Stress Ratios Induced by Earthquake Ground Motions*

The Seed-Idriss (1971) simplified procedure is used to estimate the cyclic shear stress ratios ( $CSR$ ) induced by earthquake ground motions, at a depth  $z$  below the ground surface, using the following expression:

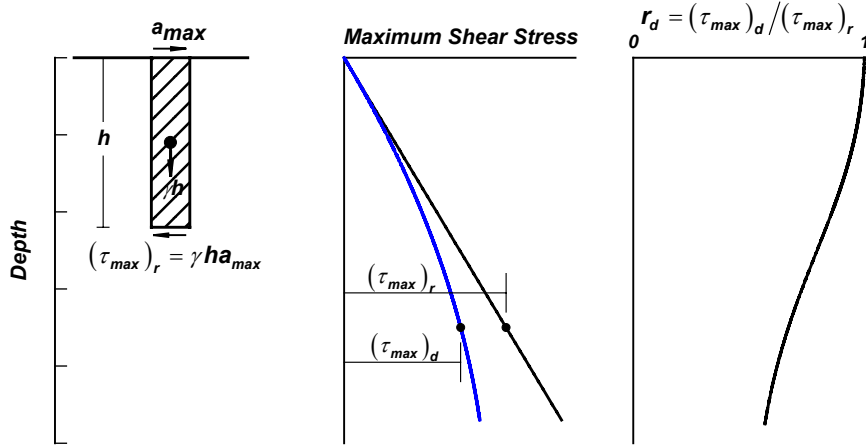


Fig. 1: Schematic for determining maximum shear stress,  $\tau_{max}$ , and the stress reduction coefficient,  $r_d$ .

$$CSR = 0.65 \left( \frac{\sigma_{vo} a_{max}}{\sigma'_{vo}} \right) r_d \quad (1)$$

in which  $a_{max}$  is the maximum horizontal acceleration at the ground surface in g's,  $\sigma_{vo}$  is the total vertical stress and  $\sigma'_{vo}$  is the effective vertical stress at depth  $z$ . The parameter  $r_d$  is a stress reduction coefficient that accounts for the flexibility of the soil column (e.g.,  $r_d = 1$  corresponds to rigid body behavior) as illustrated in Figure 1. The factor of 0.65 is used to convert the peak cyclic shear stress ratio to a cyclic stress ratio that is representative of the most significant cycles over the full duration of loading.

#### Adjustment for the Equivalent Number of Stress Cycles in Different Magnitude Earthquakes

The values of **CSR** calculated using equation (1) pertain to the equivalent uniform shear stress induced by the earthquake ground motions generated by an earthquake having a moment magnitude  $M$ . It has been customary to adjust the values of **CSR** calculated by equation (1) so that the adjusted values of **CSR** would pertain to the equivalent uniform shear stress induced by the earthquake ground motions generated by an earthquake having a moment magnitude  $M = 7\frac{1}{2}$ , i.e.,  $(CSR)_{M=7.5}$ . Accordingly, the values of  $(CSR)_{M=7.5}$  are given by:

$$(CSR)_{M=7.5} = \frac{CSR}{MSF} = 0.65 \left( \frac{\sigma_{vo} a_{max}}{\sigma'_{vo}} \right) \frac{r_d}{MSF} \quad (2)$$

#### Use of the SPT Blow Count and CPT Tip Resistance as Indices for Soil Liquefaction Characteristics

The effective use of SPT blow count and CPT tip resistance as indices for soil liquefaction characteristics require that the effects of soil density and effective confining stress on penetration resistance be separated. Consequently, Seed et al (1975a) included the normalization of penetration resistances in sand to an equivalent  $\sigma'_{vo}$  of one atmosphere ( $1 P_a \approx 1 \text{ tsf} \approx 101 \text{ kPa}$ ) as part of the semi-empirical procedure. This normalization currently takes the form:

$$(N_1)_{60} = C_N (N)_{60} \quad (3)$$

$$q_{c1} = C_N q_c \quad (4)$$

in which the  $(N)_{60}$  value corresponds to the SPT  $N$  value after correction to an equivalent 60% hammer efficiency (Seed et al 1984, 1985), and  $q_c$  is the cone tip resistance. In addition,  $q_c$  is conveniently normalized by  $P_a$  to obtain a dimensionless quantity (i.e.,  $q_{c1N} = q_{c1}/P_a$ ), as suggested by Robertson and Wride (1997). The purpose of the overburden normalization is to obtain quantities that are independent of  $\sigma'_{vo}$  and thus more uniquely relate to the sand's relative density,  $D_R$ . The correlation of the cyclic stress ratio required to cause liquefaction (which will be designated as **CRR** to distinguish it from the cyclic stress ratio **CSR** induced by the earthquake ground motions) to normalized penetration resistance is thus directly affected by the choice of the  $C_N$  relation, as will be illustrated later in this paper.

*Adjustment of Cyclic Resistance for the Effects of Overburden Stress and Sloping Ground Conditions*

The cyclic resistance ratio (**CRR**) of cohesionless soil varies with effective confining stress and is affected by the presence of static driving shear stresses such as exist beneath slopes. Note that **CRR** is the cyclic stress ratio that causes liquefaction for a  $M = 7\frac{1}{2}$  earthquake as obtained from the case-history-based semi-empirical correlations. Since the semi-empirical liquefaction correlations are based primarily on data for level ground conditions and effective overburden stresses in the range of  $100 \pm$  kPa, Seed (1983) recommended that the **CRR** be corrected for these effects using the following expression:

$$\mathbf{CRR} = \mathbf{CRR}_{\sigma=1, \alpha=0} K_o K_\alpha \quad (5)$$

in which  $K_o$  is the overburden correction factor and  $K_\alpha$  is the static shear stress correction factor. Revised  $K_\alpha$  relations are described in more detail by Boulanger (2003a) and by Idriss and Boulanger (2003a,b), and are not reviewed herein.

**STRESS REDUCTION COEFFICIENT,  $r_d$** 

Seed and Idriss (1971) introduced the stress reduction coefficient  $r_d$  as a parameter describing the ratio of cyclic stresses for a flexible soil column to the cyclic stresses for a rigid soil column, as illustrated in Figure 1. They obtained values of  $r_d$  for a range of earthquake ground motions and soil profiles having sand in the upper  $15 \pm$  m ( $\approx 50$  ft) and suggested an average curve for use as a function of depth. The average curve, which was extended only to a depth of about 12 m ( $\approx 40$  ft), was intended for all earthquake magnitudes and for all profiles.

The shear stresses induced at any point in a level soil deposit during an earthquake are primarily due to the vertical propagation of shear waves in the deposit. These stresses can be calculated using analytical procedures and are particularly dependent on the earthquake ground motion characteristics (e.g., intensity and frequency content), the shear wave velocity profile of the site, and the dynamic soil properties. Idriss (1999), in extending the work of Golesorkhi (1989), performed several hundred parametric site response analyses and concluded that for the conditions of most practical interest, the parameter  $r_d$  could be adequately expressed as a function of depth and earthquake magnitude ( $M$ ). The following relation was derived using those results:

$$\ln(r_d) = \alpha(z) + \beta(z)M \quad (6a)$$

$$\alpha(z) = -1.012 - 1.126 \sin\left(\frac{z}{11.73} + 5.133\right) \quad (6b)$$

$$\beta(z) = 0.106 + 0.118 \sin\left(\frac{z}{11.28} + 5.142\right) \quad (6c)$$

in which  $z$  is depth in meters and  $M$  is moment magnitude. These equations are considered appropriate to a depth  $z \leq 34$  m. For  $z > 34$ , the following expression is more appropriate:

$$r_d = 0.12 \exp(0.22M) \quad (6d)$$

The uncertainty in  $r_d$  increases with increasing depth such that equation (6) should only be applied for depths less than about  $20 \pm$  m. Liquefaction evaluations at greater depths often involve special conditions for which more detailed analyses can be justified. For these reasons, it is recommended that **CSR** (or equivalent  $r_d$  values) at depths greater than about 20 m should be based on site response studies, providing, however, that a high quality response calculation can be completed for the site.

Plots of  $r_d$  calculated using equation (6) for  $M = 5\frac{1}{2}$ ,  $6\frac{1}{2}$ ,  $7\frac{1}{2}$  and 8 are presented in Figure 2. Also shown in this figure is the average of the range published by Seed and Idriss in 1971. The information in Figure 2 indicates that the average of the range published by Seed and Idriss is comparable to the curve calculated using equation (6) with  $M = 8$  for depths shallower than about 4 m and is comparable to the curve calculated using equation (6) with  $M = 7\frac{1}{2}$  for depths greater than about 8 m.

Seed et al (2001) proposed the use of  $r_d$  values that are not only a function of depth and earthquake magnitude, but also of the level of shaking and the average shear wave velocity over the top 40 ft ( $\approx 12$  m) of the site. It is believed that this adds another degree of complication and implied accuracy that is not warranted at this time.

Therefore, it is suggested that the use of equation (6) would provide a sufficient degree of accuracy for engineering applications and it is recommended that these equations be used in lieu of the figure originally published by Seed and Idriss (1971) or any of the equations that have been derived over the past 30 or so years based on that figure.

**MAGNITUDE SCALING FACTOR,  $MSF$** 

The magnitude scaling factor, **MSF**, has been used to adjust the induced **CSR** during earthquake magnitude  $M$  to an equivalent **CSR** for an earthquake magnitude,  $M = 7\frac{1}{2}$ . The **MSF** is thus defined as:

$$\mathbf{MSF} = \mathbf{CSR}_M / \mathbf{CSR}_{M=7.5} \quad (7)$$

Thus, **MSF** provides an approximate representation of the effects of shaking duration or equivalent number of stress cycles. Values of magnitude scaling factors were derived by combining: (1) correlations of the number of equivalent uniform cycles versus earthquake magnitude,

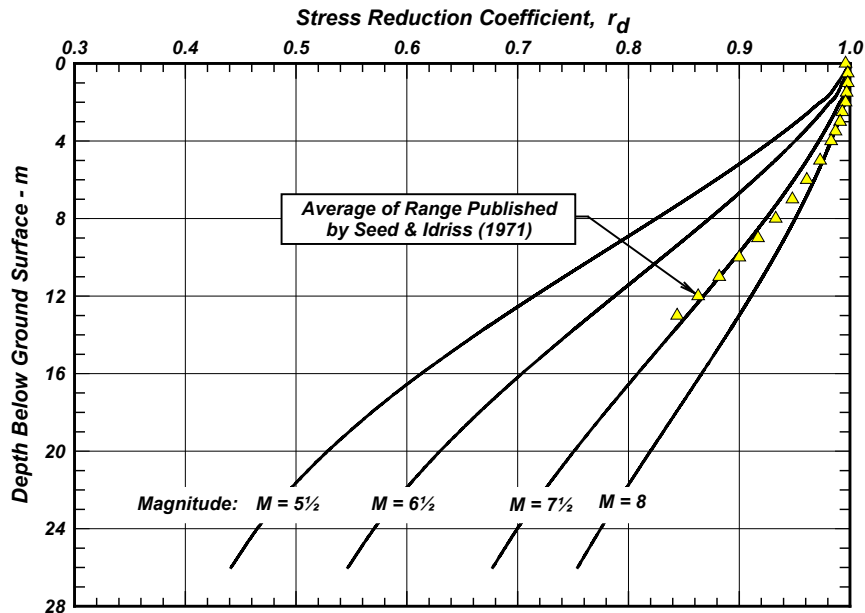


Fig. 2: Variations of stress reduction coefficient with depth and earthquake magnitude (from Idriss 1999).

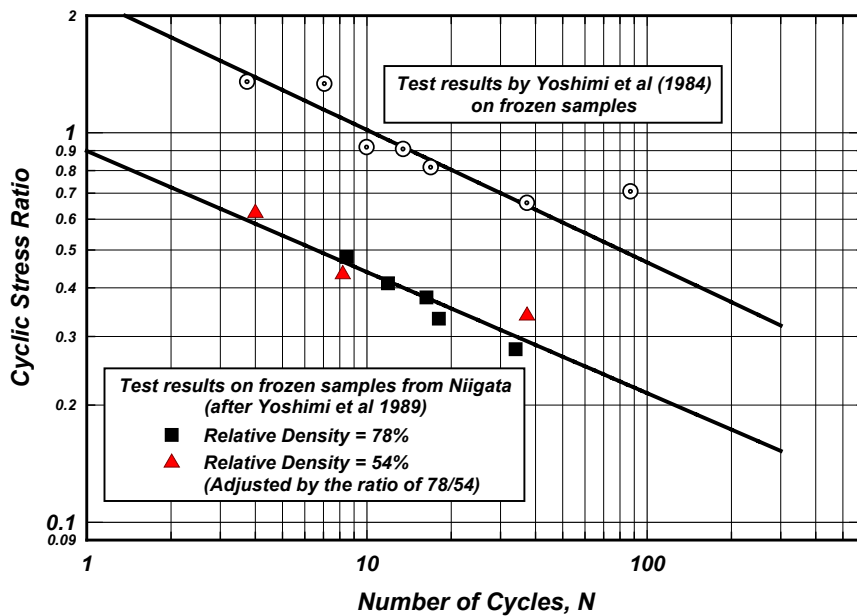


Fig. 3: Cyclic stress ratio to cause liquefaction versus number of uniform loading cycles for frozen samples tested by Yoshimi et al (1984, 1989).

and (2) laboratory-based relations between the cyclic stress ratio required to cause liquefaction and the number of uniform stress cycles. These two relations are interdependent, as described below, and thus must be developed in parallel to maintain compatibility.

Methods for converting an irregular time series to equivalent uniform cycles involve similar concepts to those used in fatigue studies. The relation between **CSR** required to cause liquefaction (i.e., **CRR**) and number of uniform stress cycles, such as shown in Figure 3, provides the means to convert the irregular stress time series into

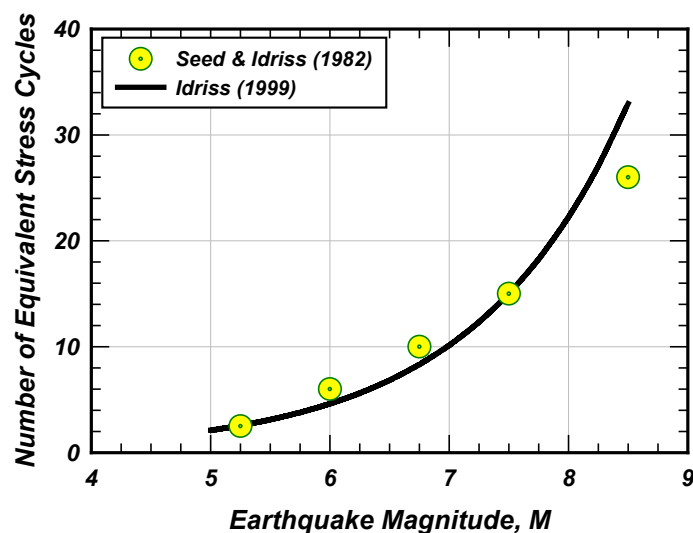


Fig. 4: Number of equivalent stress cycles versus earthquake magnitude.

an equivalent number of uniform stress cycles. For example, the data for Niigata sand in Figure 3 indicate that 10 uniform cycles at  $CRR=0.45$  would cause liquefaction, while it would take 40 uniform cycles at  $CRR=0.30$  to cause liquefaction. Thus, if an irregular stress time series consists of two cycles, one cycle with a peak of 0.45 and the other cycle having a peak of 0.30, the irregular time series can be converted to an equivalent uniform stress time series having 1.25 (i.e.,  $1 + 10/40$ ) cycles with a peak of 0.45, or 5 (i.e.,  $1 + 40/10$ ) cycles with a peak of 0.30.

This process can be carried out for any given irregular time series to represent it by an equivalent number of stress cycles each having the same peak stress. Obviously, such a conversion process depends on the relationship relating  $CRR$  and number of cycles (e.g., Figure 3). To guarantee a unique result, the curve representing  $CRR$  versus number of cycles must plot as a straight line on a log-log plot. The number of equivalent uniform cycles determined for any given irregular stress time series, therefore, depends on the slope of this line.

Idriss (1999) re-evaluated the  $MSF$  derivation, as summarized in Figures 3 through 6. Results of cyclic tests on high quality samples obtained by frozen sampling techniques were used to define the variation in  $CRR$  with the number of uniform loading cycles, as shown in Figure 3. The two sets of test results shown in Figure 3 have essentially the same slope on the  $\log(CRR)$  versus  $\log(N)$  plot, and therefore will produce comparable estimates for the equivalent number of uniform cycles produced by earthquakes of different magnitudes, and thus comparable  $MSF$  relations. In comparison, the original Seed and Idriss (1982)  $MSF$  values were based on data for reconstituted sands that had significantly lower cyclic strengths than for these field samples and a different slope

on a  $\log(CRR)$  versus  $\log(N)$  plot. Despite these differences, the re-evaluated relation for the number of equivalent uniform stress cycles versus earthquake magnitude turned out to be only slightly different from the Seed et al (1975b) results, as shown in Figure 4. The relations in Figures 3 and 4 were then used to derive the curve in Figure 5, wherein  $CRR$  was further normalized by the  $CRR$  value for 15 uniform stress cycles, which is the number of cycles obtained for  $M = 7\frac{1}{2}$  as shown in Figure 4.

The  $MSF$  relation produced by this re-evaluation was then expressed by Idriss (1999) as:

$$MSF = 6.9 \exp\left(\frac{-M}{4}\right) - 0.058 \quad (8a)$$

$$MSF \leq 1.8 \quad (8b)$$

The values of  $MSF$  obtained using equation (8) are presented in Figure 6, together with those proposed by others. The re-evaluated  $MSF$  values are somewhat greater than those originally proposed by Seed and Idriss (1982) and to those more recently derived by Cetin et al (2000) and summarized in Seed et al (2001, 2003). The relations by Ambraseys (1988), and Arango (1996) give significantly larger  $MSF$  values for earthquake magnitudes  $M < 7$ , but these differences are partly attributable to differences in the assumed  $r_d$  relations, as described below.

$MSF$  and  $r_d$  relations are inter-related through their dependence on earthquake magnitude. For example, smaller earthquake magnitudes result in smaller  $r_d$  values and larger  $MSF$  values. Consequently, empirical derivations of  $MSF$  that rely on magnitude-independent  $r_d$  relations (e.g., Ambraseys 1988, Arango 1996) are

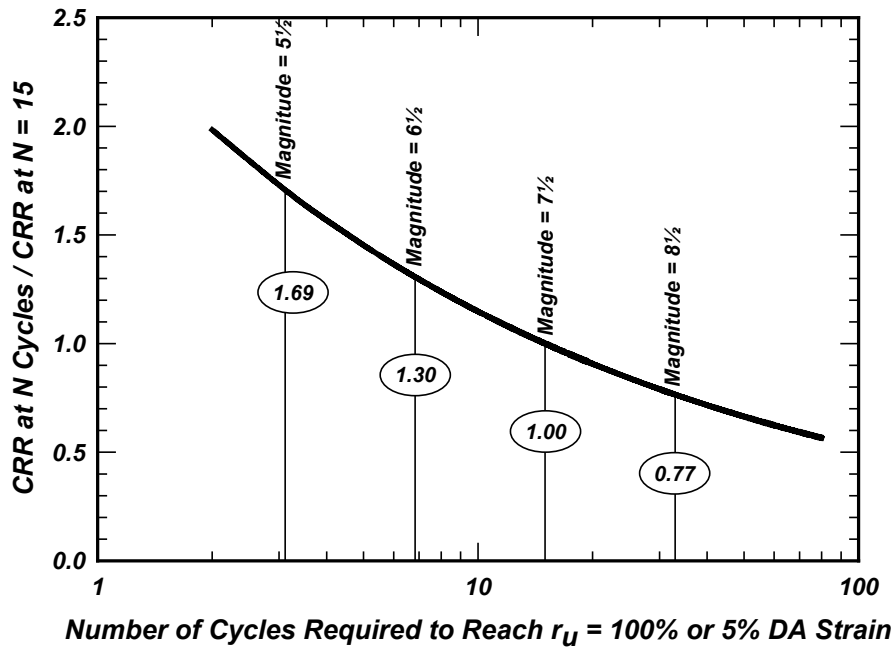


Fig. 5: Derivation of *MSF* for various earthquake magnitudes based on laboratory cyclic test data on frozen samples.

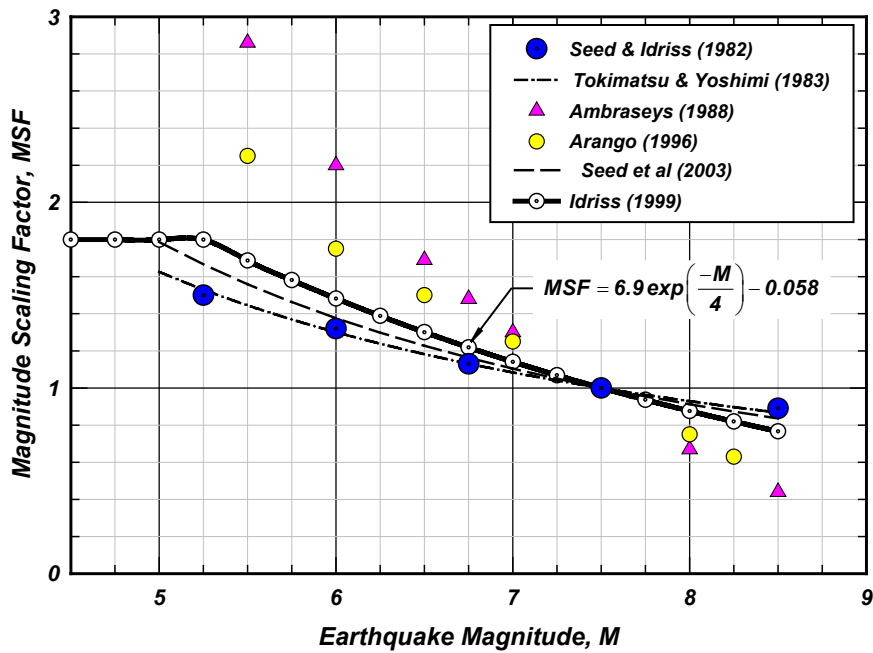


Fig. 6: Magnitude scaling factor, *MSF*, values proposed by various investigators.

lumping both effects of earthquake magnitude into the *MSF* parameter alone. For this reason, it is essential that  $r_d$  and *MSF* relations be used in the same combination in which they were derived. However, even if the *MSF*

relationships by Ambraseys (1988) or Arango (1996) are used with their corresponding magnitude-independent stress reduction coefficients, it is believed that they will

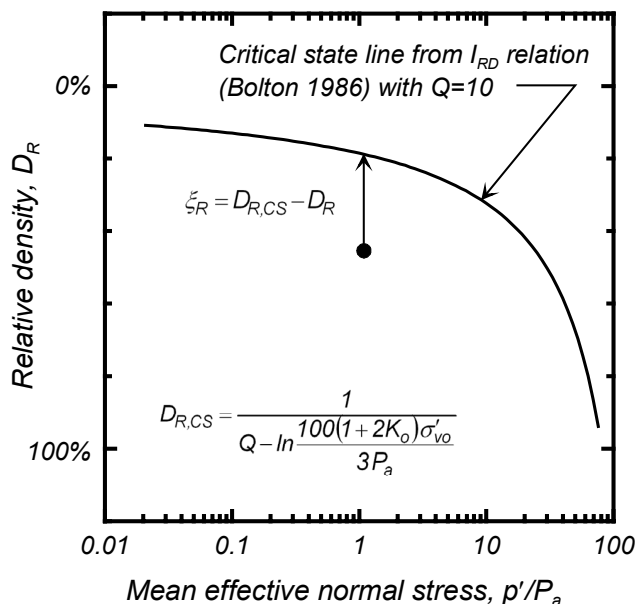


Fig. 7: Definition of the relative state parameter index (after Boulanger 2003a).

produce unconservative results for shallow depths during small magnitude earthquakes (say,  $M \leq 6\frac{1}{2}$ ).

The *MSF* relation by Idriss (1999) is limited to a maximum value of 1.8 at small earthquake magnitudes ( $M \leq 5\frac{1}{4}$ ). This limit arises from consideration of the effects of one single peak in the cyclic shear stress time series. For an earthquake dominated by one single strong cycle of shaking, the equivalent uniform cyclic loading can be no smaller than  $\frac{1}{2}$  to 1 cycle (say, an average of  $\frac{3}{4}$  cycle) at the peak cyclic stress. The *CSR* from equation (2), however, is still calculated as 0.65 times the peak shear stress. Keeping this aspect in mind, the data in Figure 3 can be extrapolated to  $N = \frac{3}{4}$  cycle to obtain the ratio:

$$\frac{(\tau_{uniform}/\sigma'_{vo})_{N=3/4}}{(\tau_{uniform}/\sigma'_{vo})_{N=15}} = 2.77 \quad (9)$$

The maximum value of the *MSF* is therefore limited by:

$$MSF \leq 0.65 \left( \frac{(\tau_{max}/\sigma'_{vo})_{N=3/4}}{0.65(\tau_{max}/\sigma'_{vo})_{N=15}} \right) \quad (10)$$

$$MSF \leq 0.65 \times 2.77 = 1.8 \quad (11)$$

The  $r_d$  and *MSF* relations described in equations (6) (8), and (11) are recommended for use in practice because they incorporate the primary features of behavior identified by analytical and experimental studies, without becoming too complex or implying undue accuracy. The actual behavior is considerably more complicated,

including the observations by Liu et al (2001) regarding the dependence of *MSF* on distance from the rupture source, the earlier work of Yoshimi et al (1989) showing a dependence of *MSF* on  $D_R$ , and the recent work by Seed et al (2001, 2003) indicating the influence of the level of shaking and stiffness of the profile on  $r_d$ . Nonetheless, it is believed that incorporating these refinements into the semi-empirical procedure introduces more complexity than is warranted at this time.

#### OVERBURDEN CORRECTION FACTOR, $K_\sigma$

The effect of overburden stress on *CRR* was recently re-evaluated in some detail by Boulanger (2003b) and Boulanger and Idriss (2004). This re-evaluation used a critical state framework in which a relative state parameter index ( $\xi_R$ ), as defined in Figure 7, was introduced as a practical means to inter-relate the combined effects of  $D_R$  and  $\sigma'_{vo}$  on *CRR* (Boulanger 2003a). As shown in Figure 7,  $\xi_R$  is the difference between the current  $D_R$  and the critical state  $D_R$  (denoted  $D_{R,CS}$ ) for the same mean effective normal stress. The critical state line in Figure 7 was derived from Bolton's (1986) relative dilatancy index ( $I_{RD}$ ), which is an empirical index that embodies critical state concepts. The parameter  $Q$  determines the stress at which the critical state line curves sharply downwards, indicating the onset of significant particle crushing, and its value depends on grain type, with  $Q \approx 10$  for quartz and feldspar (Bolton 1986). The resulting  $\xi_R$  parameter enables the



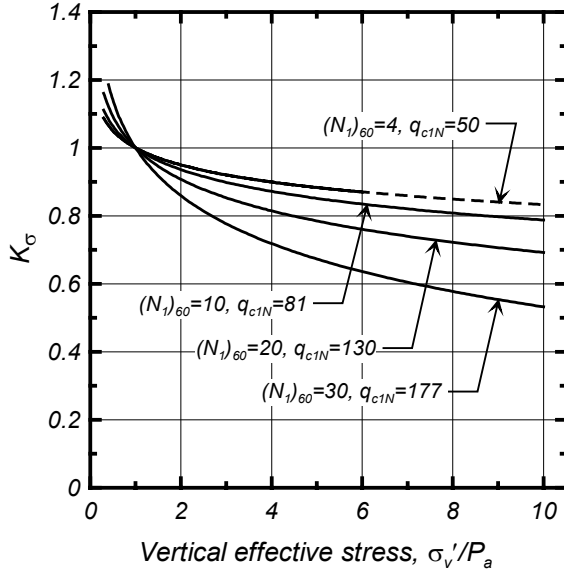


Fig. 8:  $K_\sigma$  relations derived from  $\xi_R$  relations (from Boulanger and Idriss 2004).

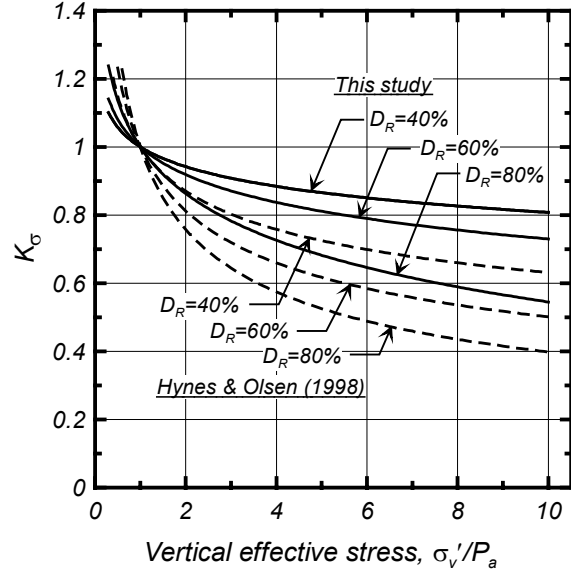


Fig. 9: Comparison of derived  $K_\sigma$  relations to those recommended by Hynes and Olsen (1998) (from Boulanger and Idriss 2004).

incorporation of critical state concepts into the analytical framework that is used to evaluate liquefaction potential. Boulanger (2003b) showed that **CRR** could be expressed as a unique function of  $\xi_R$ , and Idriss and Boulanger (2003a) showed that  $\xi_R$  could be expressed in terms of SPT or CPT penetration resistance.

The studies described above showed that overburden stress effects on **CRR** could be represented in either of two ways: (1) through the additional normalization of penetration resistances for relative state, thereby producing the quantities  $(N_1)_{60}$  and  $q_{c1N}$ , or (2) through a  $K_\sigma$  factor. In the first approach, the normalization for relative state is in addition to the conventional normalization for overburden stress [equations (3) and (4)] and it eliminates the need for a  $K_\sigma$  factor. The first approach has several technical advantages, while the second approach has been the standard approach since 1983. More details regarding the use of either approach are given in Boulanger and Idriss (2004), and are not repeated here. Instead, only the resulting relations for  $K_\sigma$  are summarized because they can more easily be compared to the methods currently in use.

The recommended  $K_\sigma$  curves are expressed as (after Boulanger and Idriss 2004):

$$K_\sigma = 1 - C_\sigma \ln \left( \frac{\sigma'_{vo}}{P_a} \right) \leq 1.0 \quad (12)$$

$$C_\sigma = \frac{1}{18.9 - 17.3D_R} \leq 0.3 \quad (13)$$

Idriss and Boulanger (2003a) re-evaluated correlations between  $(N_1)_{60}$ ,  $q_{c1N}$  and  $D_R$  for the purpose of liquefaction evaluations, and recommended the following expressions for clean sands:

$$D_R = \sqrt{\frac{(N_1)_{60}}{46}} \quad (14)$$

$$D_R = 0.478 (q_{c1N})^{0.264} - 1.063 \quad (15)$$

Boulanger and Idriss (2004) subsequently expressed the coefficient  $C_\sigma$  in terms of  $(N_1)_{60}$  or  $q_{c1N}$  as:

$$C_\sigma = \frac{1}{18.9 - 2.55\sqrt{(N_1)_{60}}} \quad (16)$$

$$C_\sigma = \frac{1}{37.3 - 8.27(q_{c1N})^{0.264}} \quad (17)$$

with  $(N_1)_{60}$  and  $q_{c1N}$  limited to maximum values of 37 and 211, respectively, in these expressions (i.e., keeping  $C_\sigma \leq 0.3$ ).

The resulting  $K_\sigma$  curves, calculated using equations (12), (13), (16) and (17), are shown in Figure 8 for a range of  $(N_1)_{60}$  and  $q_{c1N}$ . Although it is recommended that  $K_\sigma$  be restricted to  $\leq 1$  for use with the liquefaction evaluation procedures developed herein [equation (12)], the  $K_\sigma$  curves are shown without this restriction in Figures 8 and 9. The recommended  $K_\sigma$  relations provide significantly higher  $K_\sigma$  values at  $\sigma'_{vo}/P_a > 1$  and lower  $K_\sigma$  values at  $\sigma'_{vo}/P_a < 1$  in comparison to the  $K_\sigma$  curves developed by

Hynes and Olsen (1998) and recommended in Youd et al (2001), as shown in Figure 9.

The  $K_\sigma$  values were restricted to  $\leq 1$  [equation (12)] for the re-evaluation of the SPT and CPT liquefaction correlations presented later, although conceptually the  $K_\sigma$  values should be allowed to exceed 1.0 when  $\sigma'_{vo}/P_a$  is less than unity. The reasons for imposing this restriction on  $K_\sigma$  are as follows. First, the primary purpose of the  $K_\sigma$  relation is for the extrapolation of the semi-empirical correlations to depths beyond which the empirical data are available, and thus the  $K_\sigma$  relations were derived to most closely match the  $\xi_R$ -based analysis results for  $1 < \sigma'_{vo}/P_a < 10$  (Boulanger and Idriss 2004). A consequence of this focus on higher confining stresses was that the derived  $K_\sigma$  relations slightly overestimate the  $\xi_R$ -based  $K_\sigma$  values at  $\sigma'_{vo}/P_a < 1$  for the relative densities of most interest. For example, for  $D_R = 50\%$  and  $\sigma'_{vo}/P_a = 0.5$ , the  $\xi_R$ -based  $K_\sigma$  value is 1.05 while equations (12) and (13) give 1.07. In contrast, the Hynes and Olsen (1998) relations give  $K_\sigma = 1.19$  and the empirical relation by Seed et al (2003) gives  $K_\sigma = 1.20$  for this case. In effect, the  $\xi_R$ -based analyses show that  $K_\sigma$  only slightly exceeds 1.0 at  $\sigma'_{vo}/P_a < 1$  because the critical state line is relatively flat at low confining stresses (Figure 7). In addition, it was subsequently found that letting  $K_\sigma$  exceed 1.0 [using equations (12) and (13) but without an upper limit of unity], caused four data points for the clean sands from shallower depths to fall somewhat below the recommended  $CRR - (N_1)_{60}$  curve. These points were not far below the curve, and would have been closer to the curve if the  $\xi_R$ -based  $K_\sigma$  values had been used. Since the effect of  $K_\sigma$  at  $\sigma'_{vo}/P_a < 1$  is generally only a few percent, and since it was desirable for the curve not to be controlled by these few points from shallower depths, it was decided to maintain the simple limit of  $K_\sigma \leq 1$ , for both re-evaluating the case histories and for use in practical applications.

#### NORMALIZATION OF PENETRATION RESISTANCES

SPT and CPT penetration resistances are routinely normalized to an equivalent  $\sigma'_{vo} = 1$  atm to obtain quantities that more uniquely relate to the relative density,  $D_R$ , of sand (i.e., they no longer depend on  $\sigma'_{vo}$ ). One of the most commonly used expressions for the overburden correction (or normalization) factor in equations (3) and (4) was proposed by Liao and Whitman (1986), viz:

$$C_N = \left( \frac{P_a}{\sigma'_{vo}} \right)^{0.5} \quad (18)$$

Boulanger (2003b) recently re-evaluated  $C_N$  relations based on theoretical and experimental data for the CPT

and experimental data for the SPT. The  $C_N$  relation for the CPT is quite well constrained by both the theoretical solutions and the calibration chamber test data against which the theoretical solutions have been calibrated. The resulting  $C_N$  relation for the CPT was accurately expressed in the form:

$$C_N = \left( \frac{P_a}{\sigma'_{vo}} \right)^m \quad (19)$$

where the exponent  $m$  was linearly dependent on  $D_R$ , as

$$m = 0.784 - 0.521 \cdot D_R \quad (20)$$

For the SPT, Boulanger (2003b) re-evaluated the calibration chamber test data by Marcuson and Bieganousky (1977a, b) using a least squares, weighted, nonlinear regression that assumed the functional form provided by Equation (19). The resulting relations are compared in Figure 10 to the SPT calibration chamber test data for the three sands studied, after adjusting each bin of SPT data to equivalent constant  $D_R$  values. This adjustment for slight variations in  $D_R$  among different SPT tests was based on the regressed  $D_R$ -versus- $(N_1)_{60}$  relation for the individual sand. The results of these SPT regression analyses are summarized in Figure 11 showing the exponent  $m$  versus  $D_R$  for the three sands. The SPT results are consistent with the CPT relation provided by equation (20) and plotted in Figure 11 for comparison. In fact, Equation (20) provides an adequate description of both the CPT and SPT data over the range of  $D_R$  values most relevant to practice.

Boulanger and Idriss (2004) subsequently used the relations in equations (14) and (15) to obtain the following expressions for determining  $C_N$ :

$$C_N = \left( \frac{P_a}{\sigma'_{vo}} \right)^\alpha \leq 1.7 \quad (21)$$

$$\alpha = 0.784 - 0.0768 \sqrt{(N_1)_{60}}$$

$$C_N = \left( \frac{P_a}{\sigma'_{vo}} \right)^\beta \leq 1.7 \quad (22)$$

$$\alpha = 1.338 - 0.249 (q_{c1N})^{0.264}$$

with  $(N_1)_{60}$  limited to a maximum value of 46 and  $q_{c1N}$  limited to a maximum value of 254 in these  $C_N$  expressions. Extrapolating the above expressions for  $C_N$  to very shallow depths (i.e.,  $\sigma'_{vo}$  values smaller than the values for which  $C_N$  was calibrated) gives  $C_N \rightarrow \infty$  as  $\sigma'_{vo} \rightarrow 0$ . Therefore, a limit must be imposed on the maximum value of  $C_N$  because of uncertainties in equations (21) and (22) at shallow depths. The NCEER/NSF workshop in 1996/98 recommended that

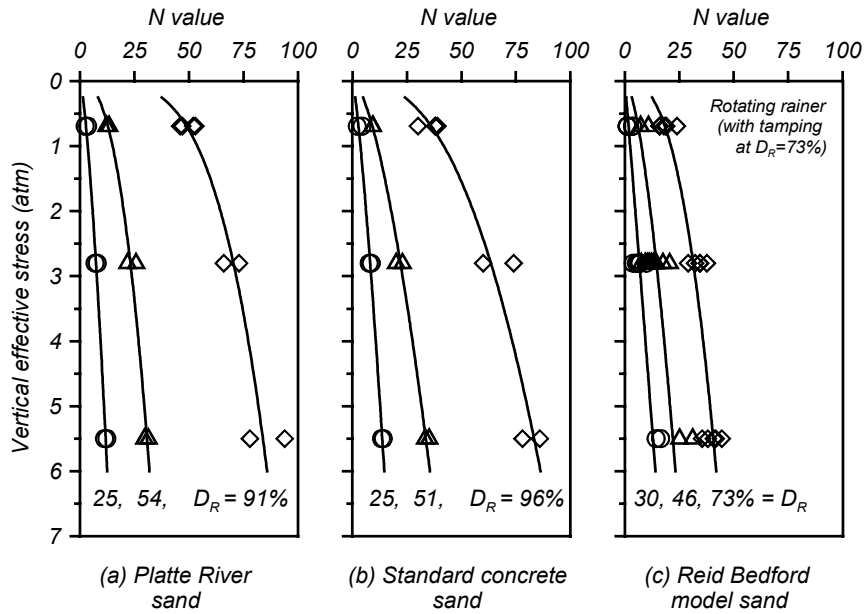


Fig. 10: Re-examination of the calibration chamber SPT data by Marcuson and Bieganousky (1977a, b) showing variation in SPT N values with vertical effective stress and relative density for three sands.

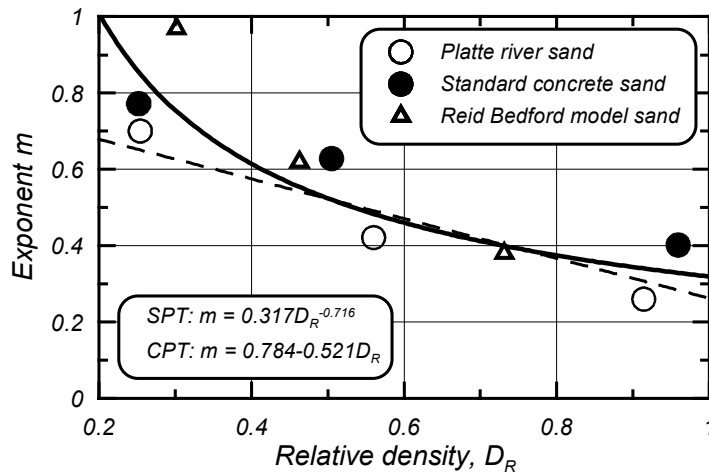


Fig. 11: Overburden normalization exponent "m" from nonlinear regression on Marcuson and Bieganousky (1977a, b) SPT calibration chamber test data and from CPT penetration theory and calibration chamber test data (Boulanger 2003b).

$C_N \leq 2$ . Considering the range of  $\sigma'_{vo}$  and  $(N)_{60}$  for the case histories of observed surface evidence of liquefaction/no-liquefaction, it would appear more reasonable to limit the value of  $C_N$  to 1.7 as noted in equations (21) and (22). The resulting  $C_N$  curves are plotted in Figure 12 showing the increasing importance of  $D_R$  with increasing depth.

Solving for  $C_N$  requires iteration because  $(N_t)_{60}$  depends on  $C_N$  and  $C_N$  depends on  $(N_t)_{60}$  (and similarly for  $q_{c1N}$ ). As suggested by Boulanger and Idriss (2004),

this iteration can be easily accomplished in most software; e.g., in Excel, use a circular reference with the "Iteration" option activated under the Tools/Options/Calculation tab.

#### SPT-BASED PROCEDURE FOR EVALUATING LIQUEFACTION POTENTIAL OF COHESIONLESS SOILS

Semi-empirical procedures for liquefaction evaluations originally were developed using the Standard Penetration Test (SPT), beginning with efforts in Japan to differentiate between liquefiable and nonliquefiable

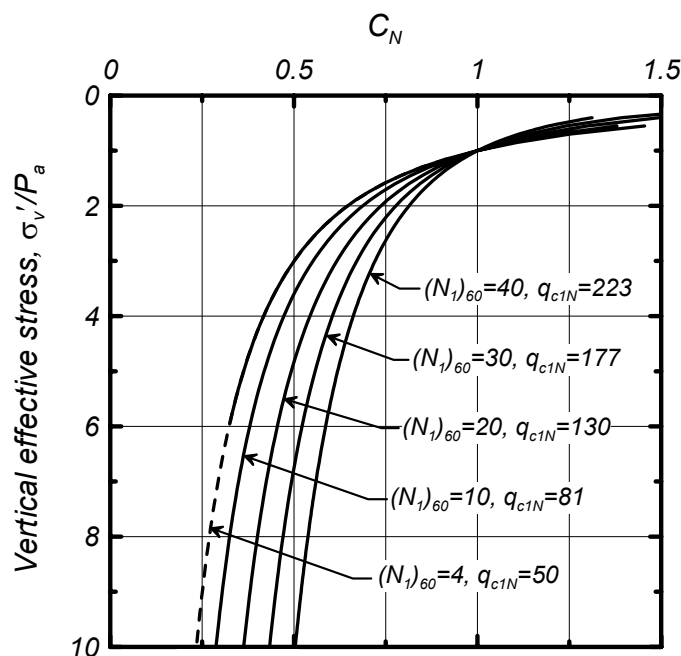


Fig. 12: Overburden normalization factor  $C_N$  calculated using equations (21) or (22) (Boulanger and Idriss 2004).

conditions in the 1964 Niigata earthquake (e.g., Kishida 1966). Subsequent developments have included contributions from many researchers, especially in the investigations of individual case histories. The procedures recommended by Seed et al (1984, 1985) to obtain and adjust the SPT blow count and to obtain the values of  $CRR$  are particularly note worthy as they have set the standard for almost two decades of subsequent engineering practice. The NCEER/NSF workshop in 1996/98 resulted in a number of suggested revisions to the SPT-based procedure but with only minor adjustments to the  $CRR - (N_1)_{60}$  curve for clean sands put forth by Seed et al (1984).

Cetin et al (2000) re-examined and expanded the SPT case history database. The data set by Seed et al (1984) had some 125 cases of liquefaction/no-liquefaction in 19 earthquakes, of which 65 cases pertain to sands with fines content  $FC \leq 5\%$ , 46 cases had  $6\% \leq FC \leq 34\%$ , and 14 cases had  $FC \geq 35\%$ . Cetin et al (2000) included an additional 67 cases of liquefaction/no-liquefaction in 12 earthquakes, of which 23 cases pertain to sands with  $FC \leq 5\%$ , 32 cases had  $6\% \leq FC \leq 34\%$ , and 12 cases had  $FC \geq 35\%$ . Cetin et al (2000) used their expanded data set and site response calculations for estimating  $CSR$  to develop revised deterministic and probabilistic liquefaction relationships. The results of Cetin et al (2000) were also summarized in Seed et al (2001).

The re-evaluation of the SPT-based procedures that is presented herein incorporates several different

adjustments and parameter revisions. The  $CSR$  and  $(N_1)_{60}$  values were re-calculated using the revised  $r_d$ ,  $MSF$ ,  $K_\sigma$ , and  $C_N$  relations recommended herein. The  $C_N$  and  $K_\sigma$  relations for silty sands were computed using the equivalent clean sand  $(N_1)_{60cs}$  values (the specific relation for this correction is described later in this section), which appears to be a reasonable approximation pending better experimental definition of how fines content affects these relations. For case histories where strong motion recordings showed that liquefaction occurred early in shaking,  $CSR$  were adjusted to reflect the number of equivalent cycles that had occurred up to the time when liquefaction was triggered (Idriss 2002). Experimental data and theoretical considerations that provide guidance on the shape of the  $CRR - (N_1)_{60}$  curve at high  $(N_1)_{60}$  values (where there is very limited case history data) were re-examined. In particular, the SPT and CPT correlations were developed in parallel to maintain consistency between the two procedures. A few additional comments on some of these aspects are provided below.

The revised  $r_d$  [equation (6)] relation was used to estimate  $CSR$  for each case history, as opposed to using site response studies. The main reason is that, except for a few cases, the available information for the liquefaction/no-liquefaction case histories is insufficient to have confidence that detailed site response analyses would be more accurate.

The  $K_\sigma$  factor is normally applied to the "capacity" side of the analysis during design [equation (5)], but it must also be used to convert the site **CSR** to a common  $\sigma'_{vo}$  value for the empirical derivation of a **CRR**– $(N_1)_{60}$  curve. This is accomplished as:

$$(\text{CSR})_{M=7.5} = 0.65 \left( \frac{\sigma_{vo} a_{max}}{\sigma'_{vo}} \right) \frac{r_d}{\text{MSF}} \frac{1}{K_\sigma} \quad (23)$$

such that the values of **CSR** correspond to an equivalent  $\sigma'_{vo}$  of 1 atm, and thus the liquefaction correlation also corresponds to an equivalent  $\sigma'_{vo}$  of 1 atm. Since  $K_\sigma$  has been restricted to  $\leq 1$  [equation (12)], this only affects a few of the case history points. Note that in applying the liquefaction correlation in design, the  $K_\sigma$  factor is still applied to the capacity side as indicated in equation (5).

The shape of the **CRR**– $(N_1)_{60}$  curve at the higher range of  $(N_1)_{60}$  values is guided by experimental and theoretical considerations because there is insufficient case history data to constrain the curve in this range. In 1982, Seed and Idriss set the **CRR**– $(N_1)_{60}$  curve asymptotic to vertical at  $(N_1)_{60} \approx 35$  because the shake table results of De Alba et al (1976) indicated that the slope of the **CRR**– $D_R$  relation would increase substantially at high values of  $D_R$ . Seed et al (1984) similarly kept the **CRR**– $(N_1)_{60}$  curve asymptotic to vertical, but at  $(N_1)_{60} \approx 30$ . In the work presented herein, the **CRR**– $(N_1)_{60}$  relation was assigned a very steep, but non-vertical, slope based on a re-evaluation of experimental results for high quality field samples obtained by frozen sampling techniques (e.g., Yoshimi et al 1984, 1989) and judgments based on theoretical considerations. In this regard, the application of probabilistic methods to the development of liquefaction correlations has often suffered from not including experimental and theoretical constraints on the liquefaction correlations at high **CRR** and  $(N_1)_{60}$  values. Consequently, such probabilistic methods often predict probabilities of liquefaction at high  $(N_1)_{60}$  values that are unreasonably high. It is believed that including experimental and theoretical findings in the development of probabilistic relations would improve the results in the upper range of **CRR** and  $(N_1)_{60}$  values.

The SPT and CPT data were utilized together in developing a consistent pair of liquefaction correlations for the cases with **FC**  $\leq 5\%$ . The consistency between the two in-situ test types was achieved through a common **CRR**– $\xi_R$  relation (Boulanger and Idriss 2004) as opposed to a constant  $q_{c1N}/N_{60}$  ratio as had been used in some past studies. Maintaining a common **CRR**– $\xi_R$  relation results in a  $q_{c1N}/N_{60}$  ratio that is dependent on  $D_R$ . The

corresponding  $q_{c1N}/(N_1)_{60}$  ratio (in lieu of  $q_{cN}/N_{60}$  ratio) can be determined using equations (14) and (15) to obtain:

$$\frac{q_{c1N}}{(N_1)_{60}} = \frac{(2.092D_R + 2.224)^{3.788}}{46(D_R)^2} \quad (24)$$

The  $q_{c1N}/(N_1)_{60}$  ratios calculated using equation (24) are plotted versus  $(N_1)_{60}$  in Figure 13, which shows values that range from greater than 10 in very loose sands to about 5.5 in very dense sands. In the range of particular interest, which is approximately  $10 \leq (N_1)_{60} \leq 25$ , the calculated  $q_{c1N}/(N_1)_{60}$  ratio ranges from 6 to 8.

The variation of the  $q_{c1N}/(N_1)_{60}$  ratio with  $D_R$  is consistent with the expected differences in drainage conditions for these two in situ tests. The CPT is a quasi-static test that is largely drained or partially drained, depending on the grain size distribution of the cohesionless soils, whereas the SPT is a dynamic test that is largely undrained. Thus, it would be expected that for SPT tests, loose sand would develop positive excess pore pressures while dense sand would more likely develop negative excess pore pressures. This difference in drainage conditions can explain, at least in part, the trend depicted in Figure 13.

Revised **CRR**– $(N_1)_{60}$  relations, derived incorporating the above considerations, are presented in Figures 14 through 19. The cases for cohesionless soils having **FC**  $\leq 5\%$  are plotted in Figure 14 along with the curve agreed to at the NCEER/NSF workshop. Also shown in Figure 14 is the new curve proposed herein. The individual cases are those from Seed et al (1984) and Cetin et al (2000) subject to the previously described adjustments. The proposed changes to the **CRR**– $(N_1)_{60}$  relation are relatively modest. For  $(N_1)_{60}$  values between 8 and 25, the maximum difference in **CRR** is about 15% at  $(N_1)_{60} \approx 20$ . The revised relation for **FC**  $\leq 5\%$  is further compared to other published relations in Figure 15, including relations from early in their development (i.e., Seed 1979) to a very recent relation by Cetin et al (2000) that is summarized in Seed et al (2001). Note that the curves and the data points for the liquefaction/no-liquefaction case histories pertain to magnitude  $M = 7\frac{1}{2}$  earthquakes and an effective vertical stress  $\sigma'_{vo} = 1$  atm ( $\approx 1$  tsf).

The cases for cohesionless soils with **FC**  $\geq 35\%$  are plotted in Figure 16 along with the applicable curve agreed to at the NCEER/NSF workshop and the new curve proposed herein. Several case history points fall well below the **FC**  $\geq 35\%$  boundary curve agreed to at the NCEER/NSF workshop, and these points control the position of the revised curve.

The **FC** =15% boundary curve that was recommended at the NCEER/NSF workshop and the revised **FC** =15% boundary curve proposed herein are compared in Figures

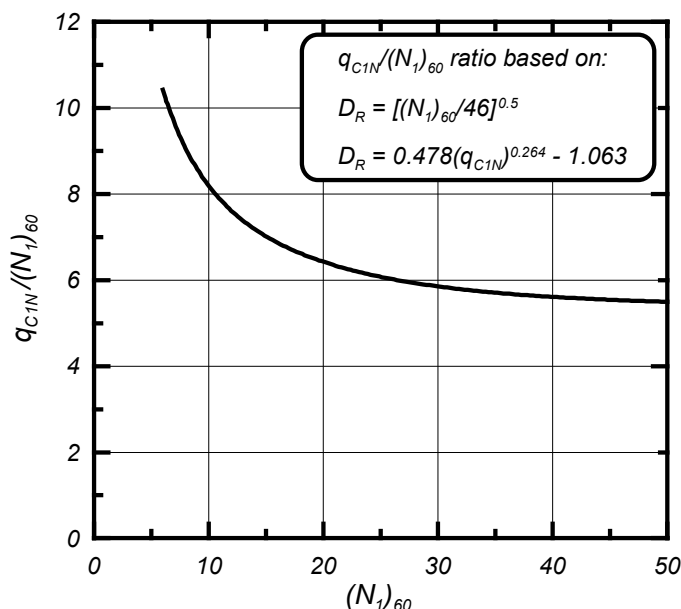


Fig. 13: Ratio of CPT and SPT penetration resistances based on adopted correlations to relative density.

17 and 18. Figure 17 shows the case history points for cohesionless soils with  $5\% < FC < 15\%$ , while Figure 18 shows the cases for  $15\% \leq FC < 35\%$ . The revised curve is lower than the curve recommended at the NCEER/NSF workshop, reflecting the influence of the revised case history data set compiled by Cetin et al (2000).

The revised boundary curves proposed herein for cohesionless soils can be expressed using the following equations. First, the SPT penetration resistance is adjusted to an equivalent clean sand value as:

$$(N_1)_{60cs} = (N_1)_{60} + \Delta(N_1)_{60} \quad (25)$$

$$\Delta(N_1)_{60} = \exp\left(1.63 + \frac{9.7}{FC} - \left(\frac{15.7}{FC}\right)^2\right) \quad (26)$$

The variation of  $\Delta(N_1)_{60}$  with  $FC$ , calculated using the equation (26), is presented in Figure 19. The value of **CRR** for a magnitude  $M=7\frac{1}{2}$  earthquake and an effective vertical stress  $\sigma'_{vo}=1$  atm ( $\approx 1$  tsf) can be calculated based on  $(N_1)_{60cs}$  using the following expression:

$$CRR = \exp\left\{ \frac{(N_1)_{60cs}}{14.1} + \left(\frac{(N_1)_{60cs}}{126}\right)^2 - \left(\frac{(N_1)_{60cs}}{23.6}\right)^3 + \left(\frac{(N_1)_{60cs}}{25.4}\right)^4 - 2.8 \right\} \quad (27)$$

The use of these equations provides a convenient means for evaluating the cyclic stress ratio required to cause

liquefaction for a cohesionless soils with any fines content.

The plasticity of the fines also likely influences the **CRR**, but an appropriate means for estimating this effect is not yet available. The approaches for evaluating the cyclic loading behavior of predominantly fine-grained soils (plastic silts or clays) are discussed in a following section. Additional research is needed to develop guidelines for evaluating the combined effects of fines content and fines plasticity on the behavior of sands. In the absence of adequate data on this issue, it is suggested that cohesionless soil behavior would include soils whose fines fraction has a plasticity index (**PI**) less than about  $5\pm$ .

It must be stressed that the quality of the site characterization work is extremely important for the reliable evaluation of liquefaction potential. With regard to SPT testing, it is vital that the testing procedures carefully adhere to established standards (as summarized at the NCEER Workshop 1997) and that, regardless of the test procedures, SPT tests can produce misleading  $(N_1)_{60}$  values near contacts between soils of greatly differing penetration resistances (e.g., sand overlying soft clay) and can miss relatively thin critical strata. Such difficulties have been reported in many cases (e.g., Boulanger et al 1995, 1997) and are generally recognized as requiring careful diligence in the field investigations. In this regard, companion CPT soundings are extremely valuable, whenever possible, for identifying SPT  $(N_1)_{60}$  values that might have been adversely affected by overlying or underlying strata, and for enabling a more reliable characterization of thin liquefiable strata (e.g., Robertson and Wride 1997, Moss 2003).

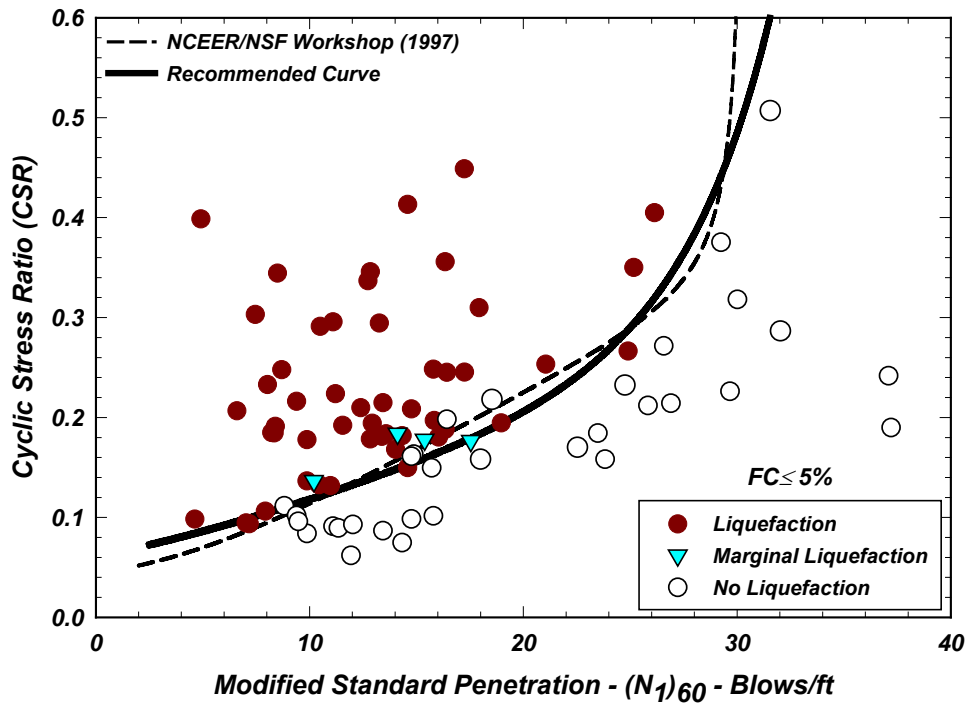


Fig. 14: SPT case histories of clean sands with the curve proposed by the NCEER Workshop (1997) and the recommended curve for  $M = 7\frac{1}{2}$  and  $\sigma'_{vo} = 1 \text{ atm} (\approx 1 \text{ tsf})$ .

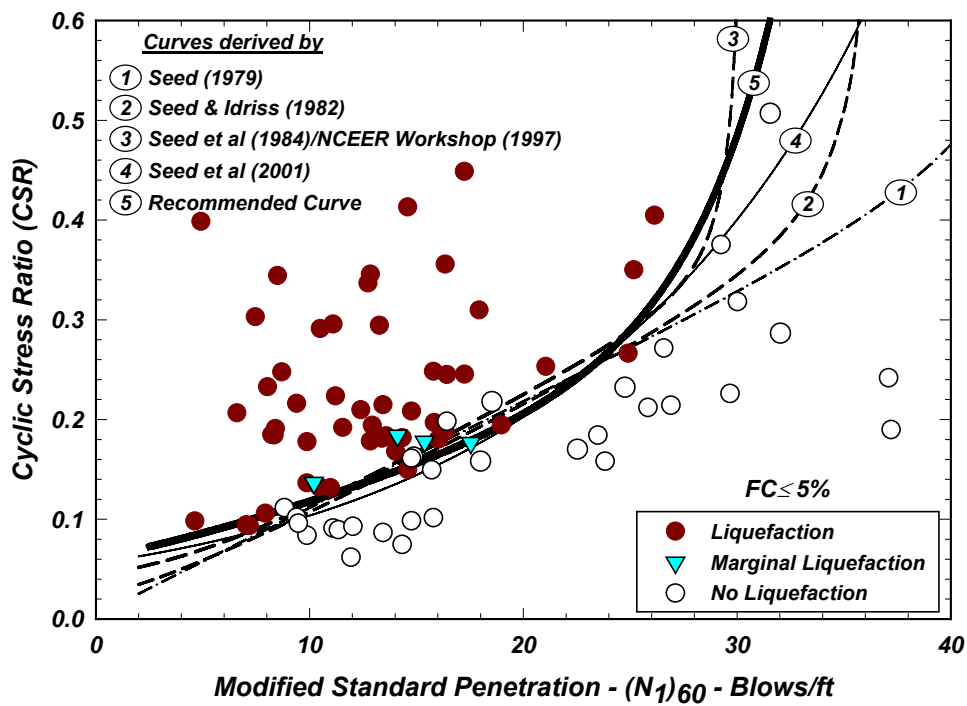


Fig. 15: Curves relating  $CRR$  to  $(N_1)_{60}$  published over the past 24 years for clean sands and the recommended curve for  $M = 7\frac{1}{2}$  and  $\sigma'_{vo} = 1 \text{ atm} (\approx 1 \text{ tsf})$ .

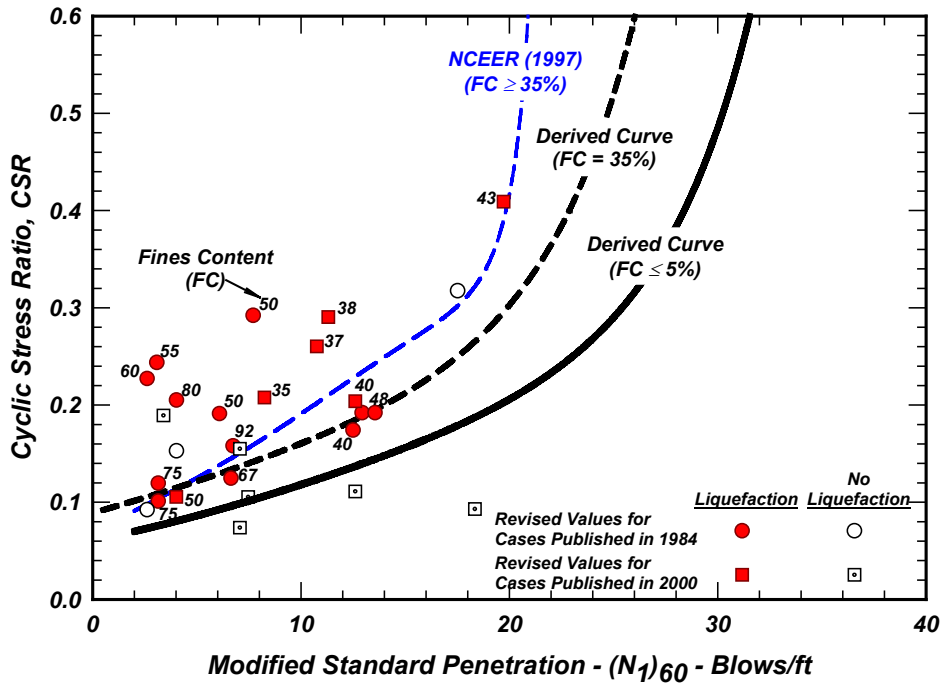


Fig. 16: SPT case histories of cohesionless soils with  $FC \geq 35\%$  and the NCEER Workshop (1997) curve and the recommended curves for both clean sand and for  $FC = 35\%$  for  $M = 7\frac{1}{2}$  and  $\sigma'_{vo} = 1 \text{ atm } (\approx 1 \text{ tsf})$ .

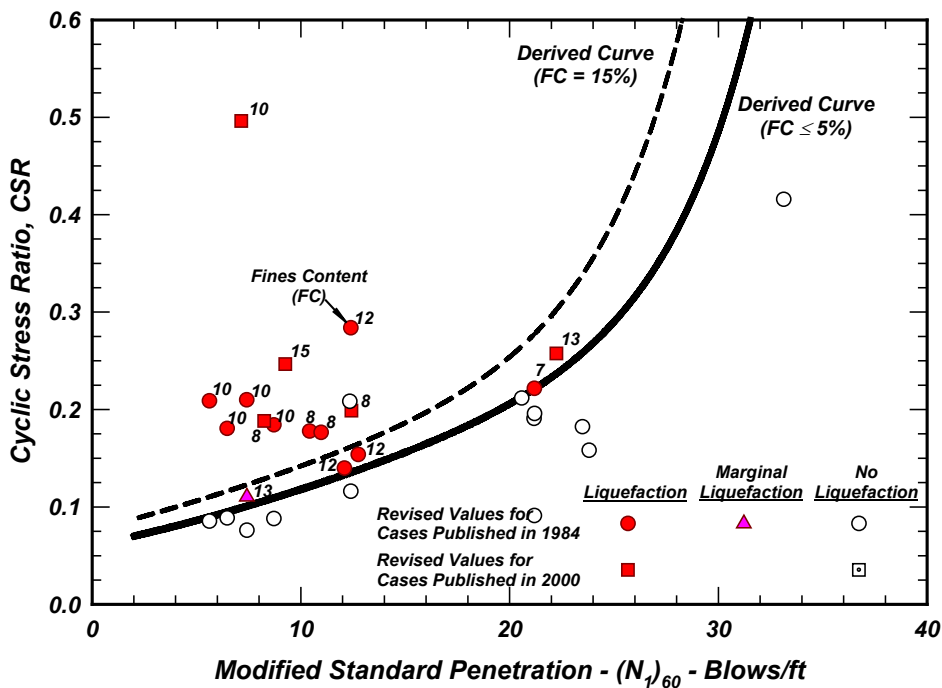


Fig. 17: SPT case histories of cohesionless soils with  $5\% < FC < 15\%$  and the recommended curves for both clean sands and for  $FC = 15\%$  for  $M = 7\frac{1}{2}$  and  $\sigma'_{vo} = 1 \text{ atm } (\approx 1 \text{ tsf})$ .



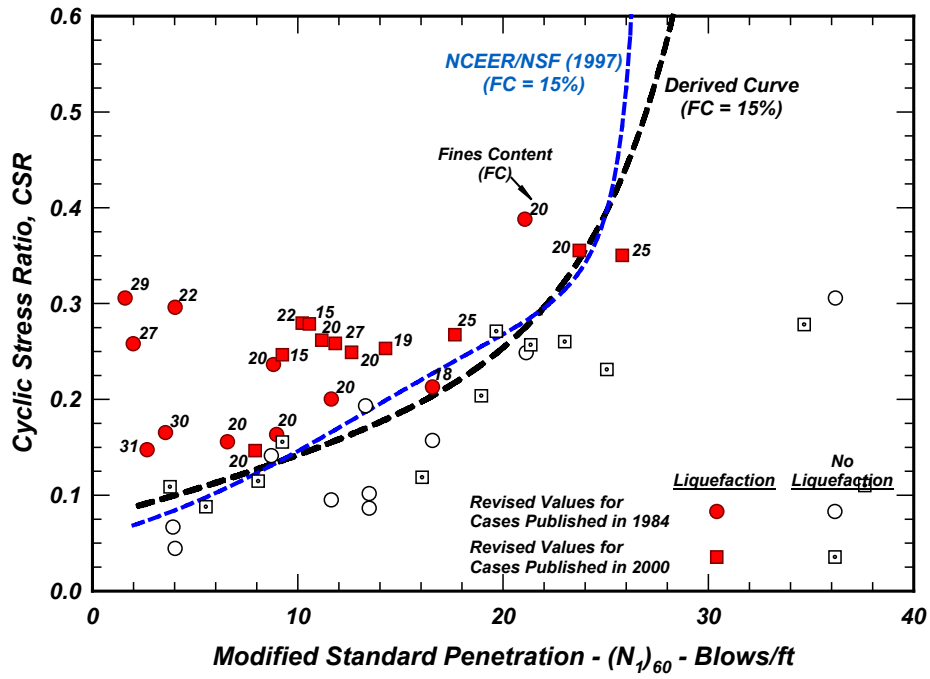


Fig. 18: SPT case histories of cohesionless soils with  $15\% \leq FC < 35\%$  and the NCEER Workshop (1997) curve and the recommended curve for  $FC = 15\%$  for  $M = 7\frac{1}{2}$  and  $\sigma'_{vo} = 1 \text{ atm} (\approx 1 \text{ tsf})$ .

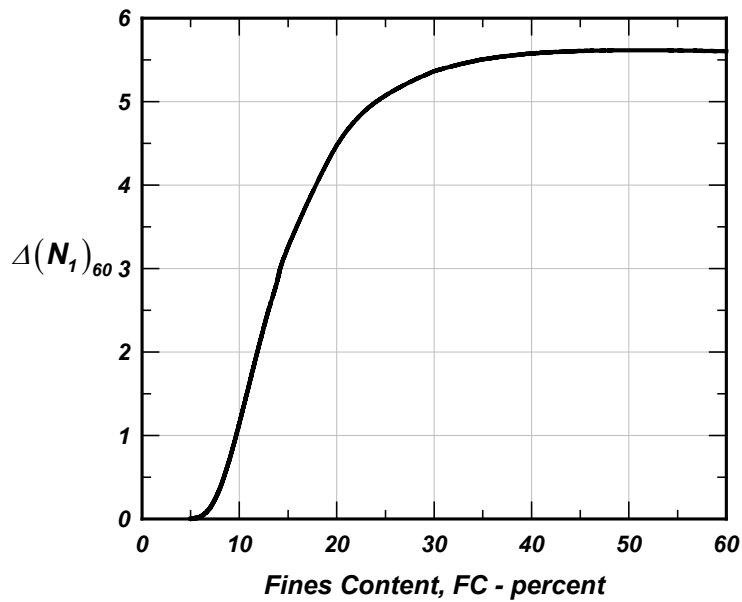


Fig. 19: Variation of  $\Delta(N_1)_{60}$  with fines content.

### CPT-BASED PROCEDURE FOR EVALUATING LIQUEFACTION POTENTIAL OF COHESIONLESS SOILS

The Cone Penetration Test (CPT) has proven to be a valuable tool in characterizing subsurface conditions and in assessing various soil properties, including estimating the potential for liquefaction at a particular site. The main advantages of using the CPT are that it provides a continuous record of the penetration resistance and is less vulnerable to operator error than is the SPT test, whereas its main disadvantage is the unavailability of a sample.

Zhou (1980) used observations from the 1978 Tangshan earthquake to propose the first liquefaction correlation based directly on CPT case histories. Seed and Idriss (1981) as well as Douglas et al (1981) proposed the use of correlations between the SPT and CPT to convert the then available SPT-based charts for use with the CPT. In recent years, the expanding data-base for field case histories has produced several CPT-based correlations (e.g., Shibata and Teparaksa 1988; Stark and Olson 1995; Suzuki et al 1995, 1997; Robertson and Wride 1997; Olsen 1997; Moss 2003; Seed et al 2003).

The CPT-based liquefaction correlation was re-evaluated by Idriss and Boulanger (2003) using case history data compiled by Shibata and Teparaksa (1988), Kayen et al (1992), Boulanger et al (1995, 1997), Stark and Olson (1995), Suzuki et al (1997), and Moss (2003). The work of Moss (2003) was particularly valuable in providing the most comprehensive compilation of field data and associated interpretations.

This re-evaluation of the CPT-based procedures incorporated adjustments and parameter revisions that are similar to those previously described for the SPT re-evaluation. For case histories where strong motion recordings showed that liquefaction occurred early in shaking,  $CSR$  were adjusted to reflect the number of equivalent cycles that had occurred up to the time when liquefaction was triggered. All  $CSR$  and  $q_{c1N}$  values were re-calculated using the revised  $r_d$ ,  $MSF$ ,  $K_\sigma$ , and  $C_N$  relations summarized above. The shape of the  $CRR - q_{c1N}$  curve at high  $q_{c1N}$  values was re-examined, and the CPT and SPT correlations were developed in parallel to maintain consistency between these procedures.

The revised  $CRR - q_{c1N}$  relation, derived using the above considerations, is shown in Figure 20 with the case history points for cohesionless soils having  $FC \leq 5\%$ . The derived relation can be conveniently expressed as:

$$CRR = \exp \left\{ \frac{q_{c1N}}{540} + \left( \frac{q_{c1N}}{67} \right)^2 - \left( \frac{q_{c1N}}{80} \right)^3 + \left( \frac{q_{c1N}}{114} \right)^4 - 3 \right\} \quad (28)$$

This  $CRR - q_{c1N}$  relation is compared in Figure 21 to those by Shibata and Teparaksa (1988), Robertson and Wride (1997), Suzuki et al (1997), and the 5% probability curve by Moss (2003) as summarized in Seed et al 2003.

The derived relation [equation (28)] is comparable to the curve proposed by Suzuki et al (1997) for clean sands. It is more conservative than the corresponding curves by Robertson and Wride (1997) and by Seed et al (2003) for almost the entire range of  $q_{c1N}$ . The curve proposed by Shibata and Teparaksa (1988) is less conservative than the derived relation except for  $q_{c1N}$  greater than about 165. Note that these relations and the plotted data pertain to magnitude  $M=7\frac{1}{2}$  earthquakes and an effective vertical stress  $\sigma'_{vo} = 1 \text{ atm} (\approx 1 \text{ tsf})$ .

As previously mentioned, the CPT and SPT liquefaction correlations were developed in parallel to maintain consistency in terms of their implied  $CRR - \xi_R$  relations for clean cohesionless soils. The relative state parameter index ( $\xi_R$ ) for a given  $q_{c1N}$  or  $(N_f)_{60}$  can be estimated using equations (14) or (15) to estimate  $D_R$ , after which  $\xi_R$  can be calculated using the expressions in Figure 7. Following this approach, the  $CRR - \xi_R$  relations produced for the SPT and CPT liquefaction correlations are compared in Figure 22. As intended, the two relations are basically identical.

The effect of fines content on the  $CRR - q_{c1N}$  relation is still being re-evaluated. This issue includes the actual effect of fines content and the most reliable means of incorporating this effect into CPT-based procedures. While revised procedures are not provided herein, a few comments regarding this issue are warranted.

Robertson and Wride (1997) and Suzuki et al (1997) suggested the use of the "soil behavior type index",  $I_c$  (Jefferies and Davies 1993), which is a function of the tip resistance ( $q_c$ ) and sleeve friction ratio ( $R_f$ ), to estimate the values of  $CRR$  for cohesionless soils with high fines content. The curve recommended by Robertson and Wride (1997) relating  $CRR - q_{c1N}$  at  $I_c = 2.59$  (defined by Robertson and Wride as corresponding to an "apparent" fines content  $FC = 35\%$ ) is presented in Figure 23. Also shown in this figure are the CPT-based data points for the cases examined by Moss (2003) for cohesionless soils with  $FC \geq 35\%$ . As can be seen in the figure, the curve recommended by Robertson and Wride (1997) is unconservative. Similarly, the relations by Suzuki et al (1997) for cohesionless soils with high fines content are unconservative. The recent work by Moss (2003) using friction ratio  $R_f$  in lieu of the parameter  $I_c$  as a proxy for fines content appears promising, but does require further scrutiny before it is adopted.

Direct soil sampling should always be the primary means for determining grain characteristics for the purpose of liquefaction evaluations. The use of CPT data alone for determining grain characteristics can lead to unreliable results in many cases, particularly when dealing with soils in the transitional range between silty sand and silty clay.

Automated analysis procedures for liquefaction evaluations using CPT data must be carefully checked for

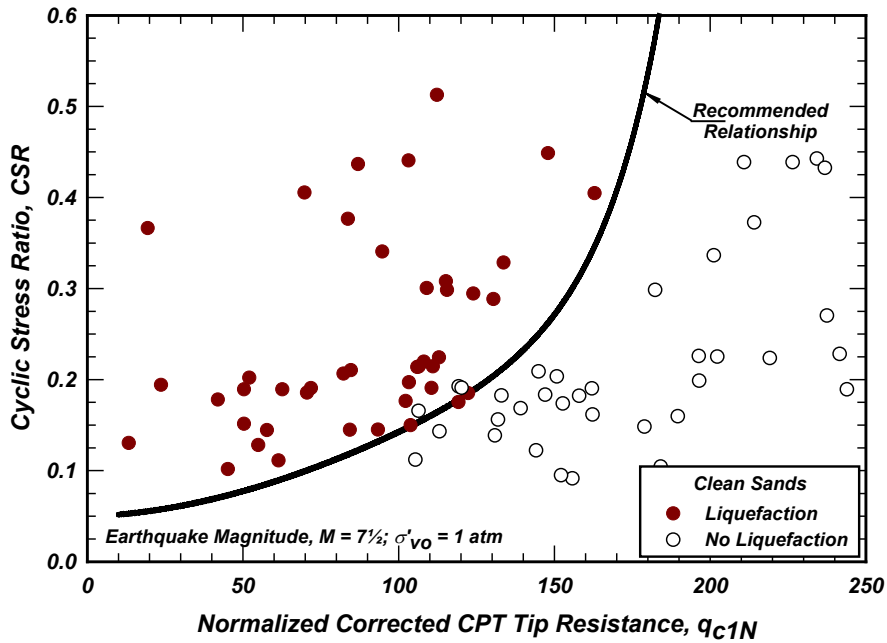


Fig. 20: CPT-based case histories and recommended relation for clean sands for  $M = 7\frac{1}{2}$  and  $\sigma'_{vo} = 1 \text{ atm}$  ( $\approx 1 \text{ tsf}$ ).

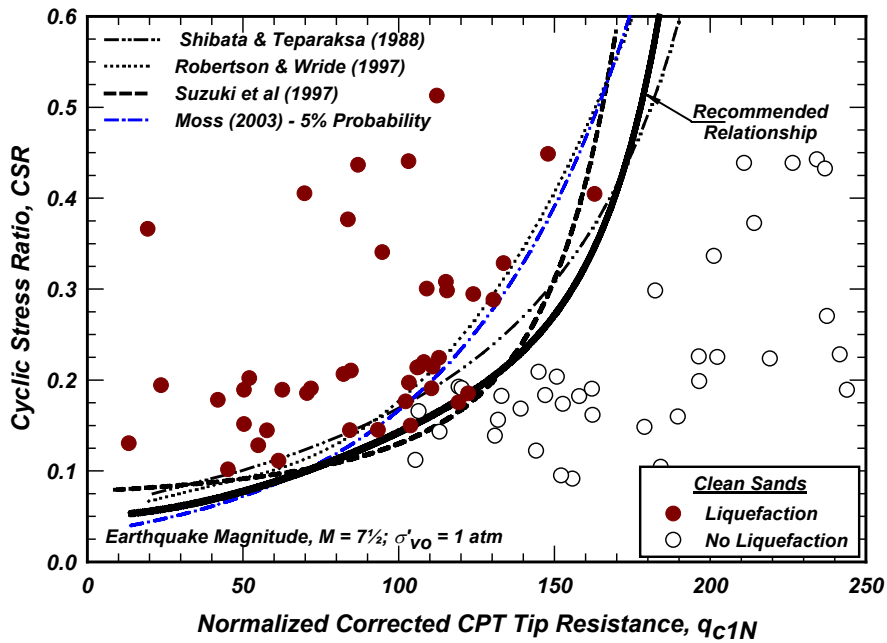


Fig. 21: CPT-based case histories and recommended relation for clean sands with relations proposed by others.

potentially misleading results near contacts between soils of greatly different penetration resistances and in finely inter-layered soils. Measurements of  $q_c$  and  $R_f$  near such contacts are not representative of the actual soil conditions, and the point-by-point liquefaction analysis of

such data is more likely to produce meaningless results than not.

The various difficulties that can be encountered using CPT-only procedures, and the steps needed to avoid these difficulties, were illustrated by Boulanger et al (1999) and

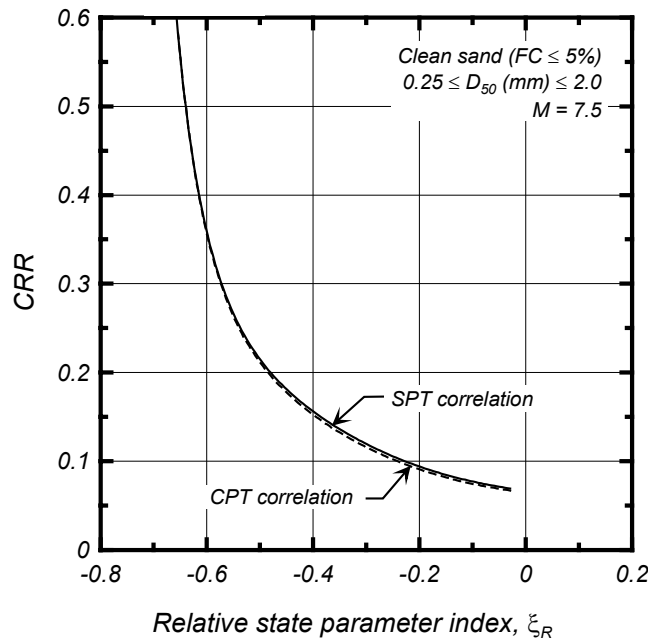


Fig. 22: Field  $CRR - \xi_R$  relations derived from liquefaction correlations for SPT and CPT.

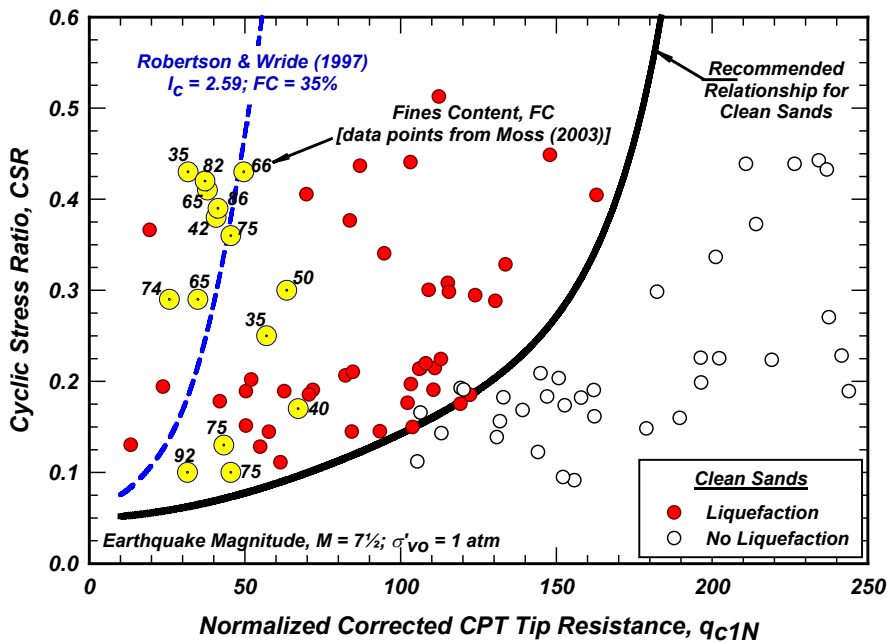


Fig. 23: Comparison of field case histories for cohesionless soils with high fines content and curve proposed by Robertson & Wride (1997) for soils with  $I_c = 2.59$  (apparent  $FC = 35\%$ )

Kulasingam et al (1999) in their analyses of the CPT soundings that were adjacent to the slope inclinometers at Moss Landing in the 1989 Loma Prieta earthquake. The three slope inclinometers were located at different positions along a sloping shoreline that spread laterally

toward the adjacent channel. The displacement profiles from the inclinometers identify the intervals over which significant shear strains, and hence liquefaction, appear to have developed. Subsequent comparisons of predicted and observed soil displacement profiles provided clear

examples of the types of difficulties/limitations that can be encountered with automated CPT-only analysis procedures. Fortunately, many of the common errors can be avoided by explicit consideration of soil sample data and site stratigraphy.

#### **$V_s$ -BASED PROCEDURE FOR EVALUATING LIQUEFACTION POTENTIAL OF COHESIONLESS SOILS**

The shear wave velocity ( $V_s$ ) based procedure has advanced significantly in recent years, with improved correlations and more complete databases, as recently summarized by Andrus and Stokoe (2000) and Andrus et al (2003). This procedure can be particularly useful for sites underlain by difficult to penetrate or sample soils (e.g., gravels, cobbles, boulders). As such,  $V_s$ -based correlations provide a valuable tool that ideally is used in conjunction with SPT- or CPT-based liquefaction correlations if possible. The question that arises, however, is which methodology should be given greater weight when parallel analyses by SPT, CPT, and/or  $V_s$  procedures produce contradictory results.

SPT, CPT, and  $V_s$  measurements each have their particular advantages and disadvantages for liquefaction evaluations, but a particularly important point to consider is their respective sensitivity to the relative density,  $D_r$ , of the cohesionless soil under consideration. For example, changing the  $D_r$  of a clean sand from 30% to 80% would be expected to increase the SPT blow count by a factor of about 7.1 and the CPT tip resistance by a factor of about 3.3 as indicated by equations (14) and (15), respectively. In contrast, the same change in  $D_r$  would be expected to only change the  $V_s$  by a factor of roughly 1.4 based on available correlations. For example, Seed and Idriss (1970) suggested the parameter  $K_{2max}$  would be 34 and 64 for  $D_r$  of 30% and 80%, respectively, which give  $V_s$  values that vary by a factor of  $\sqrt{64/34} = 1.37$ . It is likely that this range will be somewhat larger for gravelly soils.

Given that  $D_r$  is known to have a strong effect on the cyclic and post-cyclic loading behavior of saturated sand, it appears that  $V_s$  measurements would be the least sensitive for distinguishing among different types of behavior. For this reason, it may be more appropriate to view the  $V_s$  case history data-base as providing bounds that identify conditions where liquefaction is potentially highly likely, conditions where liquefaction is potentially highly unlikely, and conditions where it is uncertain whether or not liquefaction should be expected. As such, there continues to be a need for an improved understanding of  $V_s$ -based correlations and an assessment of their accuracy relative to SPT- and CPT-based correlations. In the mean time, it is recommended that greater weight be given to the results of SPT- or CPT-

based liquefaction evaluations for materials without large particle sizes.

#### **EVALUATING SEISMIC BEHAVIOR OF PLASTIC FINE-GRAINED SOILS**

Evaluating the seismic behavior of soil, whether sand or clay, requires addressing the potential for significant strains or strength loss that can contribute to ground deformations or instability during or following the occurrence of an earthquake. The procedures that are best used to estimate potential strains and strength loss during earthquake loading are different for sand than for clay, but the concerns are very similar. Unfortunately, the past literature in reference to the cyclic loading behavior of clays has not been fully interpreted in practice.

The Chinese Criteria were described by Wang (1979) and reported in Seed and Idriss (1982) as a means for identifying fine-grained soils that might be susceptible to "liquefaction". In this context, it is likely that the term liquefaction was used to describe the occurrence of ground deformations that might have been indicative of high excess pore pressures and strains in the subsurface.

Unfortunately, a classification as "nonliquefiable" by the Chinese Criteria is too often interpreted as meaning there is "no problem". This interpretation is clearly a mistake given the large body of literature describing the potential for significant strains and strength loss in plastic silts or clays during cyclic or seismic loading.

The first step in addressing the potential for seismically induced strains and strength loss in soil should instead begin with the classification of the soil as likely behaving more like a "cohesionless" soil or more like a "cohesive" soil. If the Chinese Criteria (Wang 1979) or similar index test-based criteria (e.g., Andrews and Martin 2000) are to be used, they should be viewed as an aid only for making this distinction. This distinction can often be aided by consideration of the behavior observed in consolidation tests, monotonic undrained shear strength tests, cyclic tests, and vane shear tests, for example.

If a soil is characterized as being cohesionless in behavior, then the term liquefaction refers to the class of behavior that is associated with the onset of high excess pore pressures, significant strains, and the possibility of associated strength loss. Liquefaction in the field is commonly identified by ground deformations and sand boils, while in the laboratory it may be defined more precisely in terms of some failure criterion (e.g., 3% shear strain, or  $r_u \rightarrow 100\%$ ).

If a soil is characterized as being cohesive in behavior, then the potential for cyclic strains and strength loss are identified using different procedures and the term "liquefaction" is inapplicable and should not be used to describe the behavior. Cyclic loading of clays can produce high excess pore pressures, but they are usually less than 100% by an amount that depends on the nature of the soil. For example, cyclic loading has been observed to produce  $r_u = 80-90\%$  in normally consolidated

clays (Zergoun and Vaid 1994, Boulanger et al 1998) and  $r_u \approx 75\%$  in lightly overconsolidated Bootlegger Cove clays from Anchorage (Idriss 1985). While  $r_u$  may not reach 100%, the potential for large strength loss has been clearly illustrated in lab tests (e.g., Thiers and Seed 1966) and in the field (e.g., Idriss 1985). Nonetheless, the low hydraulic conductivity of cohesive soil means that the post-earthquake dissipation of excess pore pressures is much slower and thus unlikely to produce soil/water boils. These differences in behavior ( $r_u < 100\%$  and the absence of boils) are perhaps the primary reasons why the term "liquefaction" is only used in reference to cohesionless soils.

The cyclic loading behavior of clays, or their resistance to the development of shear strains, is best evaluated in terms of the ratio of the cyclic shear stress ( $\tau_{cyc}$ ) to the undrained monotonic shear strength ( $C_u$ ). For example, the results of uniform cyclic undrained loading tests for three different saturated clays are plotted in Figure 24 in terms of the  $\tau_{cyc}/C_u$  ratio required to cause  $\pm 3\%$  strain. Note that these tests do not include any initial static driving shear stresses, which are known to have important effects on the cyclic loading behavior (e.g., Goulois et al 1985, Andersen et al 1988, Hyodo et al 1994). Results are shown for cyclic direct simple shear tests on Drammen clay at overconsolidation ratios (OCR) of 1 and 4 (Andersen et al 1988), cyclic direct simple shear tests on Boston Blue clay at OCR of 1, 1.38, and 2 (Azzouz et al 1989), and cyclic triaxial tests on normally consolidated Cloverdale clay (Zergoun and Vaid 1994). In these tests, the cyclic strains remained relatively small until the excess pore pressures built up to some critical level, after which the shear strains began to grow rapidly with each additional loading cycle. Consequently, the generation of 3% strain was closely followed by much larger strains and represents a reasonable criterion for defining cyclic strength. Note that the results in Figure 24 have been adjusted to a 1 Hz cyclic loading rate based on a 9% increase in the  $\tau_{cyc}$  required to cause 3% strain for every log-cycle of loading rate (e.g., Lefebvre and LeBoeuf 1987, Zergoun and Vaid 1994, Boulanger et al 1998), while  $C_u$  is kept at the standard rates for monotonic loading in practice. After having made this adjustment, the relation for  $\tau_{cyc}/C_u$  versus number of loading cycles ( $N$ ) appears to be very similar for different clays, as illustrated by the data in Figure 24. In addition, the data for Boston Blue clay suggests the same  $\tau_{cyc}/C_u$  versus  $N$  curve can apply to OCR of 1 to 2, while the data for Drammen clay suggests the ratio  $\tau_{cyc}/C_u$  is about 20% lower when OCR is as high as 4.

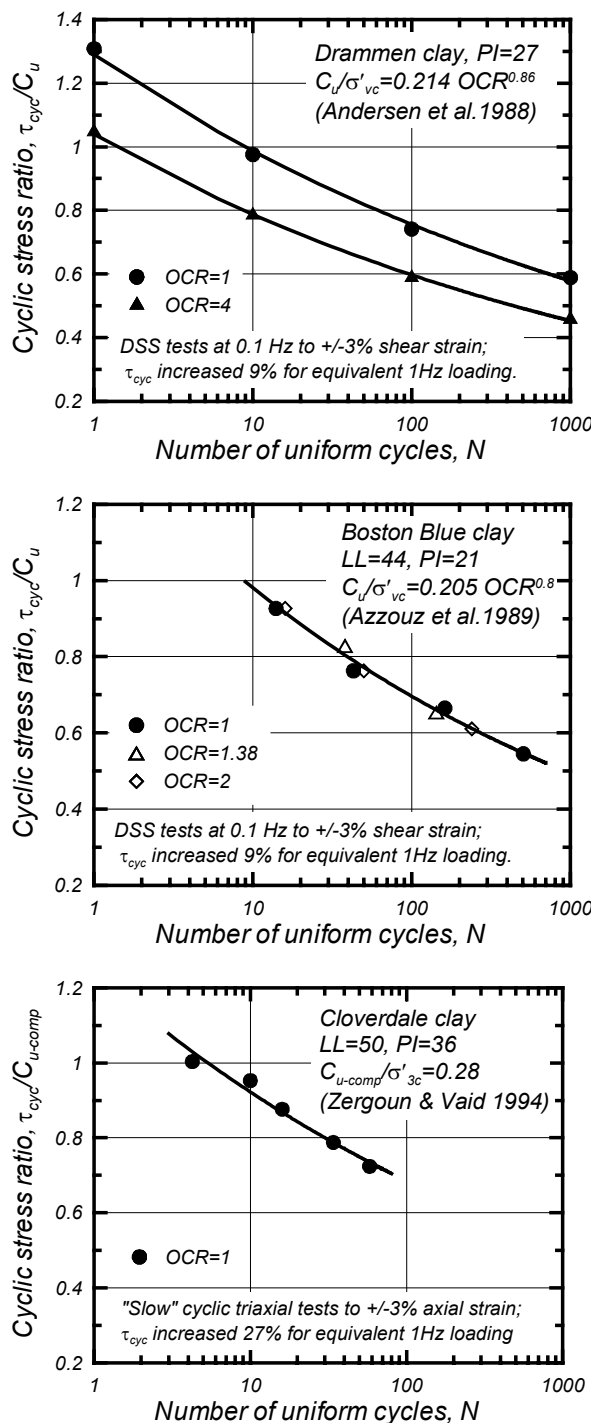


Fig. 24: Cyclic strength ratios for uniform cyclic loading of three saturated clays: (a) Drammen clay with OCR of 1 and 4; (b) Boston Blue clay with OCR of 1, 1.38, and 2; and (c) Cloverdale clay with OCR of 1.

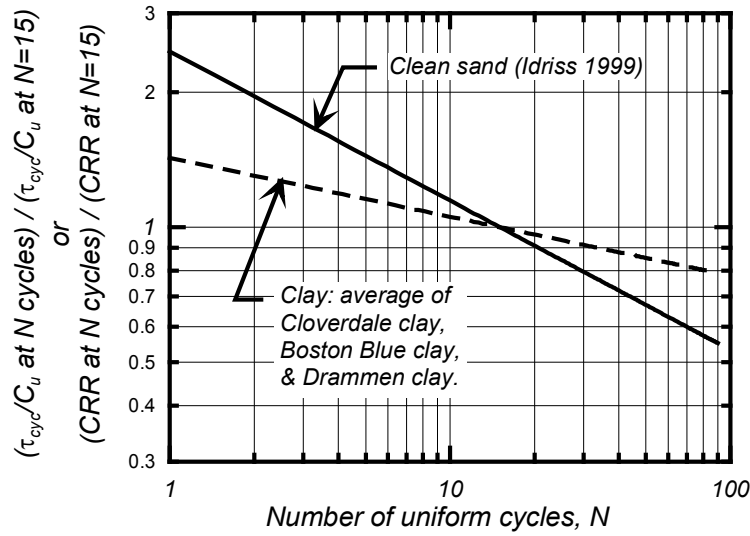


Fig. 25: Variation in cyclic strengths for clay ( $\tau_{cyc}/C_u$ ) and sand ( $CRR$ ), normalized by the cyclic strength at 15 uniform loading cycles, versus number of uniform loading cycles.

The  $\tau_{cyc}/C_u$  versus  $N$  relations in Figure 24 clearly illustrate that  $OCR$  has a strong effect on cyclic strength because of its effects on  $C_u$ . For natural deposits of cohesive soils, the approximate relation between undrained shear strength (in simple shear), vertical consolidation stress, and  $OCR$  can be expressed as (Ladd and Foott 1974):

$$C_u = \left( \frac{C_u}{\sigma'_{vc}} \right)_{NC} \sigma'_{vc} OCR^{0.8} \quad (29)$$

where  $(C_u/\sigma'_{vc})_{NC}$  is the undrained shear strength ratio for normally consolidated conditions ( $OCR=1$ ). The value of  $(C_u/\sigma'_{vc})_{NC}$  is typically equal to 0.20 to 0.24, with higher and lower values being observed for different types of silts and clays, as reported by Ladd (1991). Based on these relations, increasing  $OCR$  from 1 to 2 would be accompanied by a 74% increase in  $C_u$ . If the ratio  $\tau_{cyc}/C_u$  is unchanged by the increase in  $OCR$ , as observed for Boston Blue clay (Figure 24), then the cyclic resistance  $\tau_{cyc}$  is also increased by 74%. The importance of  $OCR$  on field behavior was well illustrated by Idriss (1985) in showing that the occurrence and nonoccurrence of landslides in Anchorage during the 1964 earthquake could be explained by the differences in  $OCR$  at different locations.

The relation between cyclic strength and number of loading cycles is significantly different for clay than for sand, and this has several important consequences on how the simplified procedure might be applied to clay. Figure 25 shows the variation in cyclic strength ratio for clay

( $\tau_{cyc}/C_u$ ) and cyclic resistance ratio for sand ( $CRR$ ), both normalized by their respective values for 15 uniform loading cycles, versus the number of uniform loading cycles. The slope of the line for the clay is much flatter than that for sand, which indicates that the behavior of the clay is much more dependent on the strongest cycles of loading in an irregular time series. In adapting the procedures previously described for sand, this means that clay will have substantially different relations for (i) equivalent number of loading cycles versus earthquake magnitude, and (ii)  $MSF$ . More detailed analyses of how to analyze clay soils within the same framework as sands, and hence facilitate simpler comparisons, are currently in progress. In the mean time, the key point is that clays can develop significant strains and deformation during earthquake loading if the level and duration of shaking are sufficient to overcome the peak resistance of the soil. If that were to happen and sufficient movement were to accrue, the strength of the soil would reduce to its residual (or remolded) strength and if the shaking continues beyond that stage, large movement would ensue. Examples of such behavior are the landslides caused by the strength loss in the Bootlegger Cove clay in downtown Anchorage in the 1964 Alaska earthquake (e.g., Idriss 1985).

There are also those soils that exhibit behavior that is intermediate to those of cohesionless and cohesive soils, and these are the most difficult to address. These soils still require further studies to develop reliable evaluation procedures. The ongoing studies of the field behavior of fine-grained soils during the 1999 Kocaeli (e.g., Sancio et al 2002) and 1999 Chi-Chi (e.g., Stewart et al 2003) earthquakes are particularly interesting.

## CONCLUDING REMARKS

An update was presented for the semi-empirical field-based procedures that are used to evaluate the liquefaction potential of cohesionless soils during earthquakes. The analytical framework upon which the case history data are organized includes several important factors, including the parameters  $r_d$ ,  $MSF$ ,  $K_\sigma$ , and  $C_N$ . The updated relations for each of these factors have a strong basis in experimental and theoretical findings, with an appropriate balance between simplicity for practice and rigor of coverage for key factors.

Revised SPT-based and CPT-based liquefaction correlations were presented that were based upon a re-examination of the field data, incorporation of the updated analytical framework, and a new approach for providing improved consistency between the two correlations. The relative roles of SPT-, CPT- and shear wave velocity-based liquefaction correlations were briefly discussed.

The procedures used to evaluate cyclic loading behavior of fine-grained soils were also discussed. Emphasis must be placed on first distinguishing whether a soil is expected to exhibit "cohesionless" or "cohesive" soil behavior, after which there are reasonably well established procedures for addressing the potential for strength loss and associated ground deformations. Classification of a soil as "nonliquefiable" by the so-called Chinese Criteria or its variants must not be equated with the absence of a problem, but rather viewed (if the Chinese Criteria were to be used) as simply indicating that the potential behavior must be evaluated by different means.

The reliability of any liquefaction evaluation depends directly on the quality of the site characterization, including the quality (and not necessarily the quantity) of the in situ and laboratory test data. The importance of quality field and laboratory work cannot be overstated, although the vital details of the various testing methods were beyond the scope of this paper. Furthermore, it is often the synthesis of findings from several different procedures that provides the most insight and confidence in making final decisions. For this reason, the practice of using a number of in situ testing methodologies, as best suited to a particular geologic setting, should continue to be the basis for standard practice, and the allure of relying on a single approach (e.g., CPT-only procedures) should be avoided.

It is hoped that the various procedures recommended herein will provide a useful and improved means for evaluating liquefaction potential in engineering practice.

## ACKNOWLEDGMENTS

The authors extend their appreciation to Drs. K. O. Cetin and R. E. S. Moss and Professor Raymond B. Seed and their colleagues in sharing their compilations of case history data and their work on liquefaction correlations as it progressed. The authors are also grateful to Professor

Jonathan P. Stewart for his valuable comments and suggestions and to Professor Kenneth H. Stokoe for his review and comments regarding the section on shear wave velocity procedures.

## REFERENCES

- [1] N. N. Ambraseys, "Engineering seismology," *Earthquake Engineering and Structural Dynamics*, 17(1), 1-105, 1988.
- [2] K. Andersen, A. Kleven, and D. Heien, "Cyclic soil data for design of gravity structures," *Journal of the Geotechnical Engineering Division*, ASCE, 114(5): 517-539, 1988.
- [3] D. C. A. Andrews, and G. R. Martin, "Criteria for liquefaction of silty soils." *Proc. 12<sup>th</sup> World Conference on Earthquake Engineering*, Auckland, New Zealand, 2000.
- [4] Andrus, R.D., Stokoe, K.H., II. "Liquefaction resistance of soils from shear-wave velocity," *Journal of Geotechnical and Geoenvironmental Engrg.*, ASCE, 126(11), 1015-1025, 2000.
- [5] Andrus, R.D., Stokoe, K.H., II, Chung, R.M., Juang, C.H. "Guidelines for evaluating liquefaction resistance using shear wave velocity measurements and simplified procedures." *NIST GCR 03-854*, National Institute of Standards and Technology, Gaithersburg, MD, 2003.
- [6] I. Arango, "Magnitude scaling factors for soil liquefaction evaluations," *J. Geotechnical Engineering*, ASCE, 122(11), 929-936, 1996.
- [7] A. S. Azzouz, A. M. Malek, and M. M. Baligh, "Cyclic behavior of clays in undrained simple shear," *Journal of the Geotechnical Engineering Div.*, ASCE, 115(5): 637-657, 1989.
- [8] M. D. Bolton, "The strength and dilatancy of sands." *Geotechnique*, 36(1), 65-78, 1986.
- [9] R. W. Boulanger, "Relating  $K_a$  to relative state parameter index." *J. Geotechnical and Geoenvironmental Engineering*, ASCE, 129(8), 770-773, 2003a.
- [10] R. W. Boulanger, "High overburden stress effects in liquefaction analyses." *J. Geotechnical and Geoenvironmental Engineering*, ASCE, 129(12), 1071-1082, 2003b.
- [11] R. W. Boulanger, I. M. Idriss, L. H. and Mejia, *Investigation and evaluation of liquefaction related ground displacements at Moss Landing during the 1989 Loma Prieta earthquake*. Report No. UCD/CGM-95/02, Center for Geotechnical Modeling, Department of Civil & Environmental Engineering, University of California, Davis, 231 pp., 1995.
- [12] R. W. Boulanger, L. H. Mejia, and I. M. Idriss, "Liquefaction at Moss Landing during Loma Prieta Earthquake." *Journal of Geotechnical and Geoenvironmental Engineering*, ASCE, 123(5): 453-467, 1997.
- [13] R. W. Boulanger, M. W. Meyers, L. H. Mejia, and I. M. Idriss, "Behavior of a fine-grained soil during Loma Prieta earthquake." *Canadian Geotechnical J.*, 35: 146-158, 1998.
- [14] R. W. Boulanger, L. H. Mejia, and I. M. Idriss, Closure to "Liquefaction at Moss Landing during Loma Prieta earthquake." *Journal of Geotechnical and Geoenvironmental Engineering*, ASCE, 125(1): 92-96, 1999.
- [15] R. W. Boulanger, and I. M. Idriss, "State normalization of penetration resistance and the effect of overburden stress on liquefaction resistance," *Proc., 11th International Conf. on Soil Dynamics and Earthquake Engineering and 3rd International Conference on Earthquake Geotechnical Engineering*, Univ. of California, Berkeley, CA, 2004.
- [16] K. O. Cetin, R. B. Seed, R. E. S. Moss, et al, "Field Case Histories for SPT-Based In Situ Liquefaction Potential Evaluation," *Geotechnical Engineering Research Report No. UCB/GT-2000/09*, Geotechnical Engineering, Department of Civil Engineering, University of California, Berkeley, 2000.
- [17] P. DeAlba, H. B. Seed, and C. K. Chan, "Sand Liquefaction in Large Scale Simple Shear Tests," *J. Geotechnical Engineering Division*, ASCE, 102(GT9), 909-927, 1976.
- [18] B. J. Douglas, R. S. Olson, and G. R. Martin, "Evaluation of the Cone Penetrometer Test for SPT Liquefaction Assessment," Pre-print 81-544, Session on In-situ Testing to Evaluate



- Liquefaction Susceptibility, ASCE National Convention, St. Louis, Missouri, October 1981.
- [19] R. Goleosorkhi, *Factors influencing the computational determination of earthquake-induced shear stresses in sandy soils*, Ph.D. thesis, University of California, Berkeley, 395 pp., 1989.
- [20] A. M. Goulois, R. V. Whitman, and K. Hoeg, "Effects of sustained shear stresses on the cyclic degradation of clay," *Strength Testing of Marine Sediments: Laboratory and In-Situ Strength Measurements*, ASTM STP 883, R. C. Chaney and K. R. Demars, eds., ASTM, Philadelphia, pp. 336-351, 1985.
- [21] M. E. Hynes and R. Olsen, "Influence of confining stress on liquefaction resistance." *Proc., Intl. Symp. on the Physics and Mechanics of Liquefaction*, Balkema, 145-152, 1998.
- [22] M. Hyodo, Y. Yamamoto, and M. Sugiyama, "Undrained cyclic shear behavior of normally consolidated clay subjected to initial static shear stress," *Soils and Foundations*, JSSMFE, 34(4), 1-11, 1994.
- [23] I. M. Idriss, "Evaluating seismic risk in engineering practice," *Proc., 11<sup>th</sup> International Conference on Soil Mechanics and Foundation Engineering*, San Francisco, Balkema, Rotterdam, 265-320, 1985.
- [24] I. M. Idriss, "An update to the Seed-Idriss simplified procedure for evaluating liquefaction potential", *Proc., TRB Workshop on New Approaches to Liquefaction*, January, Publication No. FHWA-RD-99-165, Federal Highway Administration, 1999.
- [25] I. M. Idriss, "Review of field based procedures for evaluating liquefaction potential during earthquakes." Notes from CDMG-sponsored short course on Evaluation and Mitigation of Seismic Soil Liquefaction and Seismic Slope Instability and Slope Deformation Hazards." University of California Extension, Berkeley, CA, August 8-10, 2002.
- [26] I. M. Idriss and R. W. Boulanger, "Estimating  $K_a$  for use in evaluating cyclic resistance of sloping ground." *Proc. 8<sup>th</sup> US-Japan Workshop on Earthquake Resistant Design of Lifeline Facilities and Countermeasures against Liquefaction*, Hamada, O'Rourke, and Bardet, eds., Report MCEER-03-0003, MCEER, SUNY Buffalo, N.Y., 449-468, 2003a.
- [27] I. M. Idriss and R. W. Boulanger, "Relating  $K_a$  and  $K_c$  to SPT Blow Count and to CPT Tip Resistance for Use in Evaluating Liquefaction Potential." *Proc. of the 2003 Dam Safety Conference*, ASDSO, September 7-10, Minneapolis, 2003b.
- [28] M. G. Jefferies, and M. P. Davies, "Use of CPTu to estimate equivalent SPT  $N_{60}$ ," *ASTM Geotechnical Testing Journal*, 16(4), 458-467, 1993.
- [29] R. E. Kayen, J. K. Mitchell, R. B. Seed, A. Lodge, S. Nishio, and R. Q. Coutinho, "Evaluation of SPT-, CPT-, and Shear Wave-Based Methods for Liquefaction Potential Assessments Using Loma Prieta Data," *Proc., 4<sup>th</sup> US-Japan Workshop on Earthquake Resistant Design of Lifeline Facilities and Countermeasures for Soil Liquefaction*, NCEER-92-0019, National Center for Earthquake Engineering Research, Buffalo, N.Y., pp 177-192, 1992.
- [30] H. Kishida, "Damage to Reinforced Concrete Buildings in Niigata City with Special Reference to Foundation Engineering," *Soils and Foundations*, Japanese Society of Soil Mechanics and Foundation Engineering, 7:1, 1966.
- [31] R. Kulasingam, R. W. Boulanger, and I. M. Idriss, "Evaluation of CPT liquefaction analysis methods against inclinometer data from Moss Landing." *Proc., 7<sup>th</sup> US-Japan Workshop on Earthquake Resistant Design of Lifeline Facilities and Countermeasures Against Liquefaction*, Technical Report MCEER-99-0019, MCEER, SUNY, Buffalo, 35-54, 1999.
- [32] C. C. Ladd, "Stability evaluation during staged construction," *Journal of Geotechnical Engineering*, ASCE, 117(4), 540-615, 1991.
- [33] C. C. Ladd, and R. Foott, "New design procedure for stability of soft clays." *Journal of the Geotechnical Engineering Div.*, ASCE, 100(7), 763-786, 1974.
- [34] G. Lefebvre and D. LeBoeuf, "Rate effects and cyclic loading of sensitive clays," *Journal of Geotechnical Engineering*, ASCE, 113(5), 476-489, 1987.
- [35] S. C. Liao and Whitman, R. V., "Overburden correction factors for SPT in sand." *Journal of Geotechnical Engineering*, ASCE, 112(3), 373-377, 1986.
- [36] A. H. Liu, J. P. Stewart, N. A. Abrahamson, and Y. Moriwaki, "Equivalent Number of Uniform Stress Cycles for Soil Liquefaction Analysis," *J. Geotechnical & Geoenvironmental Engineering*, ASCE, 127(12), 1017-1026, 2001.
- [37] W. F. Marcuson, III, and W. A. Bieganousky, "Laboratory standard penetration tests on fine sands." *Journal of the Geotechnical Engineering Division*, ASCE, 103(GT6), 565-588, 1977a.
- [38] W. F. Marcuson, III, and W. A. Bieganousky, "SPT and relative density in coarse sands." *Journal of the Geotechnical Engineering Division*, ASCE, 103(GT11), 1295-1309, 1977b.
- [39] R. Moss, *CPT-based probabilistic assessment of seismic soil liquefaction initiation*, Ph.D. thesis, University of California, Berkeley, CA, 2003.
- [40] National Center for Earthquake Engineering Research (NCEER), *Proceedings of the NCEER Workshop on Evaluation of Liquefaction Resistance of Soils*, T. L. Youd and I. M. Idriss, Editors, Technical Report NCEER-97-022, 1997.
- [41] R. S. Olsen, "Cyclic liquefaction based on the cone penetrometer test," *Proc., NCEER Workshop on Evaluation of Liquefaction Resistance of Soils*, National Center for Earthquake Engineering Research, State University of New York at Buffalo, Report No. NCEER-97-0022, 225-276, 1997.
- [42] P. K. Robertson, and C. E. Wride, "Cyclic Liquefaction and its Evaluation Based on SPT and CPT," *Proc., NCEER Workshop on Evaluation of Liquefaction Resistance of Soils*, National Center for Earthquake Engineering Research, State University of New York at Buffalo, Technical Report No. NCEER-97-0022, December, pp 41-88, 1997.
- [43] P. K. Robertson, and C. E. Wride, "Evaluating cyclic liquefaction potential using the cone penetration test." *Canadian Geotechnical Journal*, 35(3), 442-459, 1998.
- [44] R. B. Sancio, J. D. Bray, J. P. Stewart, T. L. Youd, H. T. Durgunoolu, A. Onalp, R. B. Seed, C. Christensen, M. B. Baturay, and T. Karadayilar, "Correlation between ground failure and soil conditions in Adapazari, Turkey," *International Journal of Soil Dynamics and Earthquake Engineering*, 22(9-12), 1093-1102, 2002.
- [45] H. B. Seed, "Soil liquefaction and cyclic mobility evaluation for level ground during earthquakes." *J. Geotechnical Engineering Division*, ASCE, 105(GT2), 201-255, 1979.
- [46] H. B. Seed, "Earthquake resistant design of earth dams." *Proc., Symposium on Seismic Design of Embankments and Caverns*, Pennsylvania, ASCE, N.Y., pp. 41-64, 1983.
- [47] H. B. Seed, and I. M. Idriss, "Soil moduli and damping factors for dynamic response analysis," Report EERC 70-10, University of California, Earthquake Engineering Research Center, Berkeley, CA, 1970.
- [48] H. B. Seed, and I. M. Idriss, "Simplified Procedure for Evaluating Soil Liquefaction Potential." *J. Soil Mechanics and Foundations Div.*, ASCE, 97:SM9, 1249-1273, 1971.
- [49] H. B. Seed, K. Mori, and C. K. Chan, "Influence of Seismic History on the Liquefaction Characteristics of Sands," Report No. EERC 75-25, Earthquake Engineering Research Center, University of California, Berkeley, August 1975a.
- [50] H. B. Seed, I. M. Idriss, F. Makdisi, and N. Banerjee, "Representation of Irregular Stress Time Histories by Equivalent Uniform Stress Series in Liquefaction Analyses," Report No. EERC 75-29, Earthquake Engineering Research Center, University of California, Berkeley, October 1975b.
- [51] H. B. Seed, and I. M. Idriss, "Evaluation of Liquefaction Potential of Sand Deposits Based on Observations of Performance in Previous Earthquakes," Pre-print 81-544, Session on In-situ Testing to Evaluate Liquefaction Susceptibility, ASCE National Convention, St. Louis, Missouri, October 1981.
- [52] H. B. Seed, and I. M. Idriss, *Ground motions and soil liquefaction during earthquakes*, Earthquake Engineering Research Institute, Berkeley, CA, 134 pp., 1982.
- [53] H. B. Seed, K. Tokimatsu, L. F. Harder, Jr., and R. Chung, "The Influence of SPT Procedures on Soil Liquefaction Resistance Evaluations," Report No. UCB/EERC-84/15, Earthquake

- Engineering Research Center, University of California, Berkeley, 1984.
- [54] H. B. Seed, K. Tokimatsu, L. F. Harder, Jr., and R. Chung, "Influence of SPT procedures in soil liquefaction resistance evaluations." *J. Geotechnical Engineering*, ASCE, 111(12), 1425-1445, 1985.
- [55] R. B. Seed, K. O. Cetin, R. E. S. Moss, A. Kammerer, J. Wu, J. Pestana, and M. Riemer, "Recent advances in soil liquefaction engineering and seismic site response evaluation," *Proc., 4<sup>th</sup> International Conference and Symposium on Recent Advances in Geotechnical Earthquake Engineering and Soil Dynamics*, Univ. of Missouri, Rolla, Paper SPL-2, 2001.
- [56] R. B. Seed, K. O. Cetin, R. E. S. Moss, A. Kammerer, J. Wu, J. Pestana, M. Riemer, R. B. Sancio, J. D. Bray, R. E. Kayen, and A. Faris, "Recent advances in soil liquefaction engineering: A unified and consistent framework." Keynote presentation, 26<sup>th</sup> Annual ASCE Los Angeles Geotechnical Spring Seminar, Long Beach, CA, 2003.
- [57] T. Shibata, and W. Teparaksa, "Evaluation of liquefaction potentials of soils using cone penetration tests," *Soils and Foundations*, Tokyo, Japan, 28(2), pp 49-60, 1988.
- [58] T. D. Stark, and S. M. Olson (1995), "Liquefaction Resistance Using CPT and Field Case Histories," *Journal of Geotechnical Engineering*, ASCE, 121(12), 856-869, 1995.
- [59] J. P. Stewart, D. B. Chu, S. Lee, J. S. Tsai, P. S. Lin, B. L. Chu, R. E. S. Moss, R. B. Seed, S. C. Hsu, M. S. Yu, and M. C. H. Wang, "Liquefaction and non-liquefaction from 1999 Chi-Chi, Taiwan, earthquake," *Advancing Mitigation Technologies and Disaster Response for Lifeline Systems*, Technical Council on Lifeline Earthquake Engineering, Monograph No. 25, J. E. Beavers ed., 1021-1030, 2003.
- [60] Y. Suzuki, K. Tokimatsu, Y. Taya, Y. Kubota, "Correlation Between CPT Data and Dynamic Properties of In Situ Frozen Samples," *Proceedings, Third International Conference on Recent Advances in Geotechnical Earthquake Engineering and Soil Dynamics*, Vol. 1, St. Louis, Missouri, 1995.
- [61] Y. Suzuki, K. Koyamada, and K. Tokimatsu, "Prediction of Liquefaction Resistance Based on CPT Tip Resistance and Sleeve Friction," *Proceedings, 14<sup>th</sup> International Conference on Soil Mechanics and Foundation Engineering*, Hamburg, Germany, Vol. 1, pp 603 – 606, 1997.
- [62] G. R. Thiers, and H. B. Seed, "Cyclic stress-strain characteristics of clays," *J. Soil Mechanics and Foundations Div.*, ASCE, 94(2), 555-569, 1968.
- [63] K. Tokimatsu, and Y. Yoshimi, "Empirical correlation of soil liquefaction based on SPT N-value and fines content," *Soils and Foundations*, JSSMFE, 23(4), 56-74, 1983.
- [64] Wang, W. S., "Some findings in soil liquefaction." Water Conservancy and Hydroelectric Power Scientific Research Institute, Beijing, China, 1979.
- [65] Y. Yoshimi, K. Tokimatsu, O. Kaneko, and Y. Makihara, "Undrained cyclic shear strength of a dense Niigata sand," *Soils and Foundations*, JSSMFE, 24(4), 131-145, 1984.
- [66] Y. Yoshimi, K. Tokimatsu, Y. Hosaka, "Evaluation of liquefaction resistance of clean sands based on high quality undisturbed samples." *Soils and Foundations*, JGS, 29(11), 93-104, 1989.
- [67] T. L. Youd et al., "Liquefaction resistance of soils: Summary report from the 1996 NCEER and 1998 NCEER/NSF workshops on evaluation of liquefaction resistance of soils." *J. Geotech. and Geoenviron. Engrg.*, ASCE, 127(10), 817-833, 2001.
- [68] M. Zergoun, and Y. P. Vaid, "Effective stress response of clay to undrained cyclic loading," *Canadian Geotechnical Journal*, 31: 714-727, 1994.
- [69] S. Zhou, "Evaluation of the Liquefaction of Sand by Static Cone penetration Test," *Proceedings, 7<sup>th</sup> World Conference on Earthquake Engineering*, Istanbul, Turkey, Vol. 3, 1980.